PROCEEDINGS A

rspa.royalsocietypublishing.org

Research

Cite this article: Nitschke I, Nestler M, Praetorius S, Löwen H, Voigt A. 2018 Nematic liquid crystals on curved surfaces: a thin film limit. *Proc. R. Soc. A* **474**: 20170686. http://dx.doi.org/10.1098/rspa.2017.0686

Received: 4 October 2017
Accepted: 16 May 2018

Subject Areas:
biophysics, materials science, mathematical modelling

Keywords:
nematic liquid crystals, thin film limit, surface equation

Author for correspondence:
Ingo Nitschke
e-mail: ingo.nitschke@tu-dresden.de

Nematic liquid crystals on curved surfaces: a thin film limit

Ingo Nitschke[1], Michael Nestler[1], Simon Praetorius[1], Hartmut Löwen[2] and Axel Voigt[1,3]

[1]Institut für Wissenschaftliches Rechnen, Technische Universität Dresden, 01062 Dresden, Germany
[2]Institut für Theoretische Physik II - Soft Matter, Heinrich-Heine-Universität Düsseldorf, 40225 Düsseldorf, Germany
[3]Dresden Center for Computational Materials Science (DCMS), 01062 Dresden, Germany

AV, 0000-0003-2564-3697

We consider a thin film limit of a Landau–de Gennes Q-tensor model. In the limiting process, we observe a continuous transition where the normal and tangential parts of the Q-tensor decouple and various intrinsic and extrinsic contributions emerge. The main properties of the thin film model, like uniaxiality and parameter phase space, are preserved in the limiting process. For the derived surface Landau–de Gennes model, we consider an L^2-gradient flow. The resulting tensor-valued surface partial differential equation is numerically solved to demonstrate realizations of the tight coupling of elastic and bulk free energy with geometric properties.

1. Introduction

We are concerned with nematic liquid crystals whose molecular orientation is subjected to a tangential anchoring on a curved surface. Such surface nematics offer a non-trivial interplay between the geometry and the topology of the surface and the tangential anchoring constraint which can lead to the formation of topological defects. An understanding of this interplay and the resulting type and position of the defects is highly desirable.

As an application, nematic shells have been proposed as switchable capsules optimal for a steered drug

THE ROYAL SOCIETY PUBLISHING

delivery [1]. The defect structure thereby essentially determines where the shells can be opened in a minimal destructive way. Moreover, nematic shells are possible candidates to form supramolecular building blocks for tetrahedral crystals with important implications for photonics [2].

Besides such equilibrium structures, defects also play a fundamental role in active systems. In [3], the spatio-temporal patterns that emerge when an active nematic film of microtubules and molecular motors is encapsulated within a lipid vesicle is analysed. The combination of activity, topological constraints and geometric properties produces a myriad of dynamical states. Understanding these relations offers a way to design biomimetic materials, with topological constraints used to control the non-equilibrium dynamics of active matter.

Defects in nematic shells are intensively studied on a sphere [4–10] and under more complicated constraints (e.g. [11–16]). However, most of these studies use particle methods. Despite the interest in such methods, a continuum description would be more essential for predicting and understanding the macroscopic relation between position and type of the defects and geometric properties of the surface. For bulk nematic liquid crystals, the Landau–de Gennes Q-tensor theory [17,18] is a well-established field theoretical description. For a mathematical review, we refer to [19]. However, its surface formulation is still under debate. Surface models have been postulated by analogue derivations on the surface [20], by considering the limit of vanishing thickness for bulk Q-tensors models [21,22] or via a discrete-to-continuum limit [23]. The derived models differ in details and strongly depend on the made assumptions in the derivation.

Our approach aims to derive a surface Q-tensor model by dimensional reduction via a thin film limit of a general bulk Landau–de Gennes model. In contrast to previous work, we only make assumptions on the boundary of the thin film where we admit only states conforming to critical points of the free energy. In the limiting process, we observe a continuous transformation where the normal and tangential parts of the Q-tensor decouple and various intrinsic and extrinsic contributions emerge. The obtained surface Landau–de Gennes energy is compared with that of previous models [20–23] and an L^2-gradient flow is considered. The resulting tensor-valued surface partial differential equation is solved numerically on an ellipsoid.

The paper is structured as follows. In §2, we present the main results, including the surface Landau–de Gennes energy, a formulation for the evolution problem, and numerical results to illustrate the mentioned interplay between the geometry, the topology of the surface, and the positions and type of the defects. §3 establishes the notation essential for the derivation of the thin film limit, which is derived in §4 for the energy and the L^2-gradient flow. A discussion of mathematical and physical implications of the derived model and a comparison with previously postulated thin film models is provided in §5. Conclusion is drawn in §6 and details of the analysis are given in appendix A.

2. Main results

We consider Q-tensor fields on oriented compact (smooth) Riemannian manifolds $\mathcal{M}$ defined by $\mathcal{Q}(\mathcal{M}) := \{\boldsymbol{t} \in \mathrm{T}^{(2)}(\mathcal{M}) : \operatorname{tr} \boldsymbol{t} = 0, \boldsymbol{t} = \boldsymbol{t}^{\mathrm{T}}\}$. We assume $\mathcal{M}$ as well as n-tensor bundles $\mathrm{T}^{(n)}(\mathcal{M})$ to be sufficiently smooth and consider two types of manifolds $\mathcal{M}$, a regular surface $\mathcal{S} \subset \mathbb{R}^3$ without boundaries and a thin film $\mathcal{S}_h := \mathcal{S} \times [-h/2, h/2] \subset \mathbb{R}^3$ of thickness h. We have $\mathcal{Q}(\mathcal{S}) \subset \mathcal{Q}(\mathcal{S}_h)|_{\mathcal{S}}$ and we can tie a surface Q-tensor $\boldsymbol{q} \in \mathcal{Q}(\mathcal{S})$ with a restricted bulk Q-tensor $\boldsymbol{Q} \in \mathcal{Q}(\mathcal{S}_h)|_{\mathcal{S}}$ by the orthogonal projections $\boldsymbol{\Pi} = \mathrm{Id} - \boldsymbol{\nu} \otimes \boldsymbol{\nu}$, with identity Id and surface normal $\boldsymbol{\nu}$ and $\mathrm{P}_{\mathcal{Q}}$ a Q-tensor projection defined in (4.8), i.e.

$$\boldsymbol{q} = \mathrm{P}_{\mathcal{Q}}(\boldsymbol{\Pi}\boldsymbol{Q}|_{\mathcal{S}}\boldsymbol{\Pi}) = \boldsymbol{\Pi}\boldsymbol{Q}|_{\mathcal{S}}\boldsymbol{\Pi} + \tfrac{1}{2}(\boldsymbol{\nu}\boldsymbol{Q}|_{\mathcal{S}}\boldsymbol{\nu})\boldsymbol{\Pi}. \tag{2.1}$$

For Q-tensors $Q \in \mathcal{Q}(\mathcal{S}_h)$, we consider the elastic and bulk free energy $\mathcal{F}^{\mathcal{S}_h} = \mathcal{F}^{\mathcal{S}_h}_{\text{el}} + \mathcal{F}^{\mathcal{S}_h}_{\text{bulk}}$ with

$$\left.\begin{aligned} \mathcal{F}^{\mathcal{S}_h}_{\text{el}}[Q] &:= \frac{1}{2}\int_{\mathcal{S}_h} L_1\|\nabla Q\|^2 + L_2\|\operatorname{div} Q\|^2 + L_3\langle \nabla Q, (\nabla Q)^{T_{(2\,3)}}\rangle \\ &\quad + L_6\langle (\nabla Q)Q, \nabla Q\rangle \,\mathrm{d}V \\ \text{and}\qquad \mathcal{F}^{\mathcal{S}_h}_{\text{bulk}}[Q] &:= \int_{\mathcal{S}_h} a\operatorname{tr} Q^2 + \frac{2}{3}b\operatorname{tr} Q^3 + c\operatorname{tr} Q^4 \,\mathrm{d}V, \end{aligned}\right\} \tag{2.2}$$

(e.g. [24]) with elastic parameters L_i, thermotropic parameters a, b and c and $T_{(2\,3)}$ a permutation of the second and third tensor indices, see (3.9). For simplicity, we restrict our analysis to achiral liquid crystals, i.e. $L_4 = 0$, see the general form in [24]. Owing to a proper tensor calculus, the energies (2.2) are coordinate-independent and thus can be seen as a generalization of the Euclidean coordinate case in [24], see §3 for more details.

To allow a relation to the Frank–Oseen elastic constants in the uniaxial nematic-order state, the L_6 term is considered, see [25–27]. However, it should be pointed out that such a third-order elastic energy term provides a thermodynamic incorrect theory, see [28]. Including the L_6 term makes the energy unbounded from below (e.g. [29]). We will address this issue in more detail in §5.

Let $\Pi Q \nu = \nu Q \Pi = 0$ and $\nu Q \nu = \beta$ be essential anchoring conditions at $\partial\mathcal{S}_h$, where β is considered to be constant. Consequently, we obtain the natural anchoring conditions

$$\Pi((L_1 + \beta L_6)(\nabla Q)\nu + L_3(\nabla Q)^{T_{(2\,3)}}\nu)\Pi = 0 \quad \text{at } \partial\mathcal{S}_h, \tag{2.3}$$

which ensure vanishing boundary integrals in the first variation $\delta\mathcal{F}^{\mathcal{S}_h}$. For q as in (2.1), we obtain in the thin film limit $(1/h)\mathcal{F}^{\mathcal{S}_h}[Q] = \mathcal{F}^{\mathcal{S}}[q] + \mathcal{O}(h^2)$ the corresponding surface free energy $\mathcal{F}^{\mathcal{S}} = \mathcal{F}^{\mathcal{S}}_{\text{el}} + \mathcal{F}^{\mathcal{S}}_{\text{bulk}}$ with

$$\left.\begin{aligned} \mathcal{F}^{\mathcal{S}}_{\text{el}}[q] &:= \frac{1}{2}\int_{\mathcal{S}} L_1'\|\nabla q\|^2 + L_6\langle (\nabla q)q, \nabla q\rangle \\ &\quad + M_1\operatorname{tr} q^2 + M_2\langle B, q\rangle^2 + M_3\operatorname{tr} q^2\langle B, q\rangle + M_4\langle B, q\rangle + C_0 \,\mathrm{d}\mathcal{S} \\ \text{and}\qquad \mathcal{F}^{\mathcal{S}}_{\text{bulk}}[q] &:= \int_{\mathcal{S}} a'\operatorname{tr} q^2 + c\operatorname{tr} q^4 + C_1 \,\mathrm{d}\mathcal{S}, \end{aligned}\right\} \tag{2.4}$$

and shape operator $B = -(\Pi\nabla)\nu$. In contrast to (2.2), all operators are defined by the Levi–Civita connection and inner products are considered at the surface. All parameter functions $L_1', M_1, M_2, M_3, M_4, C_0, C_1$ and a' can be related to the thin film parameters L_i, the thermotropic parameters a, b and c, the surface quantities $\mathcal{H}$ (mean curvature) and $\mathcal{K}$ (Gaussian curvature), and β, see (4.31). The L^2-gradient flow $\partial_t q = -\nabla_{L^2}\mathcal{F}^{\mathcal{S}}$ reads

$$\begin{aligned} \partial_t q = {} & L_1'\Delta^{dG} q + L_6\left((\nabla\nabla q) : q + (\nabla q)\cdot\operatorname{div} q - \frac{1}{2}(\nabla q)^{T_{(1\,3)}} : \nabla q + \frac{1}{4}\|\nabla q\|^2 g\right) \\ & - (M_1 + M_3\langle B, q\rangle + 2a' + 2c\operatorname{tr} q^2)q - \left(M_2\langle B, q\rangle + \frac{M_3}{2}\operatorname{tr} q^2 + \frac{M_4}{2}\right)\left(B - \frac{1}{2}\mathcal{H}g\right) \end{aligned} \tag{2.5}$$

on $\mathcal{S}\times[0,T]$ with the div-Grad (Bochner) Laplacian Δ^{dG}. The same evolution equation also follows as the thin film limit of the corresponding L^2-gradient flow $\partial_t Q = -\nabla_{L^2}\mathcal{F}^{\mathcal{S}_h}$ for (2.2).

To numerically solve the tensor-valued surface partial differential equation (2.5), we use a similar approach as considered in [30,31]. We reformulate the equation in $\mathbb{R}^3$ Euclidean coordinates and penalize all normal contributions $q\cdot\nu$, to enforce tangentiality of the tensor. This leads to a coupled nonlinear system of scalar-valued surface partial differential equations for the components of q, which can be solved using surface finite elements [32]. The approach is implemented in the finite-element toolbox AMDiS [33,34]. Figure 1 shows the evolution on a spheroidal ellipsoid. The initial configuration is set as in [30] (fig. 1), with two sinks, a source and a saddle defect, which are placed along an equatorial plane. In accordance with the Poincaré–Hopf theorem, the topological charges of these defects add up to the Euler characteristic of the

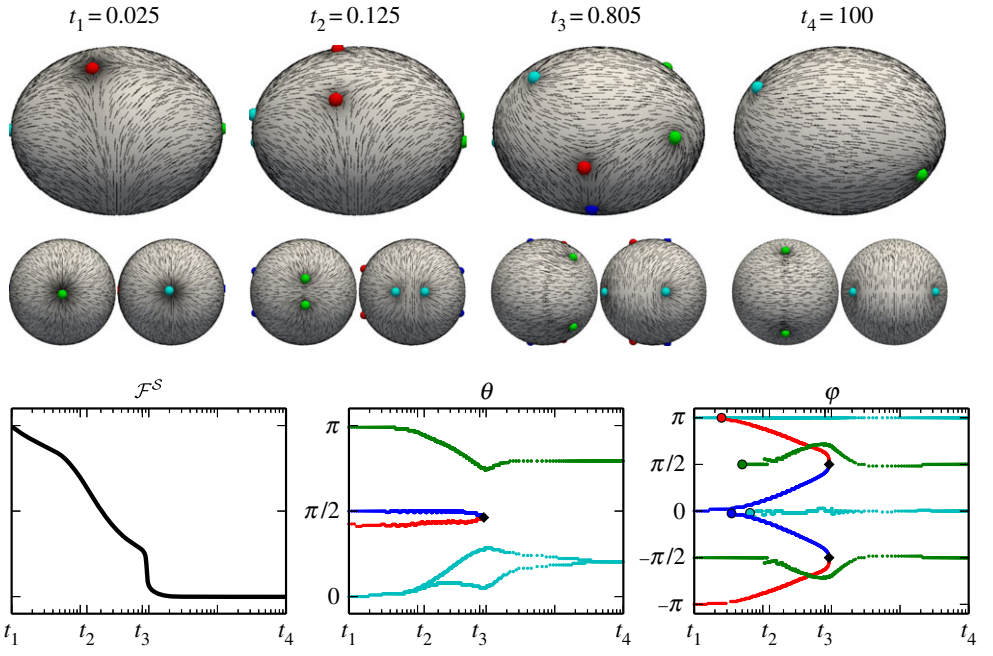

Figure 1. Numerical simulation on an ellipsoid: (top) snapshots (side, top, bottom view) of defects and principal director. From left to right: t_1: initial state of four defects, three with topological charge $+1$ (nodes: cyan, green, blue) and one with topological charge -1 (saddle node: red); t_2: break down into pairs of six $+\frac{1}{2}$ (wedges) and two $-\frac{1}{2}$ (trisectors) defects, respectively; t_3: attraction and repulsion of defects until two pairs of oppositely charged defects annihilate; t_4: minimum energy state with four $+\frac{1}{2}$ defects in deformed tetrahedral configuration as described in [20]. (bottom) From left to right: surface free-energy $\mathcal{F}^{\mathcal{S}}$ plotted over time; defect positions in spherical coordinates with polar angle θ and azimuthal angle φ over time. The colours (grey scale) correspond to the marked defects in the top row. Coloured (grey-scaled) dots mark emerging defects, black diamonds indicate defect annihilation. The half-axis of the ellipsoid are [1, 1, 1.25] and parameters are $L_1 = L_2 = -L_3 = 1$, $L_6 = 0$, $M_2 = M_3 = 0$ and $a = -\frac{2}{3}$, $b = -\frac{1}{2}$, $c = 1$. We further consider $\mathcal{F}^{\mathcal{S}} = \mathcal{F}^{\mathcal{S}}_{\text{el}} + \omega\mathcal{F}^{\mathcal{S}}_{\text{bulk}}$ with $\omega = 100$. (Online version in colour.)

surface, $1 + 1 + 1 - 1 = 2$. After some rearrangement, all four defects split into pairs of $+\frac{1}{2}$ and $-\frac{1}{2}$ defects, which move away from each other perpendicular to the initial equatorial plane. Equally charged defects repel each other and oppositely charged defects attract each other. This leads to an annihilation of two pairs of $+\frac{1}{2}$ and $-\frac{1}{2}$ defects. According to the geometric properties of the ellipsoid, the remaining four $+\frac{1}{2}$ defects arrange pairwise in the vicinity of the high curvature regions, with each pair perpendicular to each other. This deformed tetrahedral configuration is known to be the minimal energy state, see [35,36] for a sphere and [20] for ellipsoids. We further observe the principal director to be aligned with the minimal curvature lines in the final configuration. This alignment is a consequence of the extrinsic contributions in (2.4), where our model differs from previous studies. Another remarkable feature of the derived surface Landau–de Gennes model is the possibility of coexisting isotropic and nematic phases. Such coexistence is known in three-dimensional models and results from the presence of the tr $\boldsymbol{Q}^3$ term in (2.2). Such a term is absent in two-dimensional models in flat space. This difference in the three- and two-dimensional model typically changes the phase transition type. In our model the dependency of M_1 on curvature, see (4.31), allows to locally modify the double-well potential in (2.4) and thus allows for coexisting states due to changing geometric properties of the surface.

3. Notational convention and thin film calculus

For notational compactness of tensor algebra, we use the Ricci calculus, where lowercase indices $i, j, k, \ldots$ denote components in a surface coordinate system and uppercase indices $I, J, K, \ldots$ denote

components in the extended three-dimensional thin film coordinate system. Brackets [] and {} are used to switch between components and object representation, i.e. for a 2-tensor $\boldsymbol{t}$ we write $[\boldsymbol{t}]_{ij} = t_{ij}$ for the components and $\{t_{ij}\} = \boldsymbol{t}$ for the object. Most of the tensor formulations in this paper are invariant w.r.t. coordinate transformations, thus a co- and contravariant distinction in the object representation is not necessary. However, if such a distinction is needed, we use the notation of musical isomorphisms $\sharp$ and $\flat$ for raising and lowering indices, respectively. These are extended to tensors in a natural way, e.g. for a 2-tensor $\boldsymbol{t} = \{t^i{}_j\} \in \mathrm{T}^1{}_1\mathcal{S}$ we write $^\flat\boldsymbol{t}^\sharp = \{t_i{}^j\} = \boldsymbol{g}\{t^i{}_j\}\boldsymbol{g}^{-1} \in \mathrm{T}_1{}^1\mathcal{S}$ with metric tensor $\boldsymbol{g}$ in $\mathcal{S}$. Finally, a tensor product denotes a contraction $[\boldsymbol{st}]_{ij} := s_i{}^k t_{kj}$ and the Frobenius norm of a rank-n tensor $\boldsymbol{t}$ will be denoted by $\|\boldsymbol{t}\|_{\boldsymbol{g}}$, i.e. $\|\boldsymbol{t}\|_{\boldsymbol{g}}^2 = \langle \boldsymbol{t}, \boldsymbol{t}\rangle_{\boldsymbol{g}}$ with $\langle \boldsymbol{s}, \boldsymbol{t}\rangle_{\boldsymbol{g}} := s_{i_1\dots i_n} t^{i_1\cdots i_n}$ that has to be understood w.r.t. the corresponding metric $\boldsymbol{g}$ for raising and lowering the indices.[1]

The first, second and third fundamental form are denoted by $g_{ij} = \langle \partial_i \boldsymbol{x}, \partial_j \boldsymbol{x}\rangle$ (metric tensor), $[\boldsymbol{B}]_{ij} = -\langle \partial_i \boldsymbol{x}, \partial_j \boldsymbol{\nu}\rangle$ (covariant shape operator) and $[\boldsymbol{B}^2]_{ij} = \langle \partial_i \boldsymbol{\nu}, \partial_j \boldsymbol{\nu}\rangle$, respectively. With this, curvature quantities can be derived: $\mathcal{K} = \det \boldsymbol{B}^\sharp$ (Gaussian curvature) and $\mathcal{H} = \mathrm{tr}\boldsymbol{B} = \boldsymbol{B}^i{}_i$ (mean curvature). The Kronecker delta will be denoted by $\boldsymbol{\delta} = \{\delta^i_j\}$ and the Christoffel symbols (of second kind) will be denoted by $\Gamma^k_{ij} = \frac{1}{2} g^{kl}(\partial_i g_{jl} + \partial_j g_{il} - \partial_l g_{ij})$ at the surface and $\mathbb{\Gamma}^K_{IJ} = \frac{1}{2} G^{KL}(\partial_I G_{JL} + \partial_J G_{IL} - \partial_L g_{IJ})$ in the thin film, where $\boldsymbol{G}$ is the metric tensor of the thin film $\mathcal{S}_h$, e.g. $G_{IJ} = \delta_{IJ}$ and $\mathbb{\Gamma}^K_{IJ} = 0$ in the Euclidean case.

The surface $\mathcal{S}$ and the thin film $\mathcal{S}_h$ as Riemannian manifolds are equipped with different metric compatible Levi–Civita connections ∇. We use ';' in the thin film and '|' at the surface to point out the difference for covariant derivatives in index notation, e.g.

$$[\nabla \boldsymbol{Q}]_{IJK} = Q_{IJ;K} = \partial_K Q_{IJ} - \mathbb{\Gamma}^L_{KI} Q_{LJ} - \mathbb{\Gamma}^L_{KJ} Q_{IK} \quad \text{in } \mathcal{S}_h \tag{3.1}$$

and

$$[\nabla \boldsymbol{q}]_{ijk} = q_{ij|k} = \partial_k q_{ij} - \Gamma^l_{ki} q_{lj} - \Gamma^l_{kj} q_{ik} \quad \text{in } \mathcal{S}. \tag{3.2}$$

We define the coordinate in normal direction $\boldsymbol{\nu}$ of the surface $\mathcal{S}$ by $\xi \in [-h/2, h/2]$. The local surface coordinates are (u, v) defined on every chart in the atlas of $\mathcal{S}$, s.t. the immersion $\boldsymbol{x} : (u, v) \mapsto \mathbb{R}^3$ parametrize the surface. Adding these up, we obtain a parametrization $\boldsymbol{X} : (u, v, \xi) \mapsto \mathbb{R}^3$ of the thin film $\mathcal{S}_h$, defined by $\boldsymbol{X}(u, v, \xi) := \boldsymbol{x}(u, v) + \xi \boldsymbol{\nu}(u, v)$. This means, the lowercase indices $i, j, k, \dots$ are in $\{u, v\}$ and the uppercase indices $I, J, K, \dots$ are in $\{u, v, \xi\}$. The canonical choices of basis vectors in the tangential bundles are $\partial_i \boldsymbol{x} \in \mathrm{T}\mathcal{S}$ and $\partial_I \boldsymbol{X} \in \mathrm{T}\mathcal{S}_h$. Therefore, the metric tensors are defined by $g_{ij} = \partial_i \boldsymbol{x} \cdot \partial_j \boldsymbol{x}$ and $G_{ij} = \partial_I \boldsymbol{X} \cdot \partial_J \boldsymbol{X}$. Consequently, it holds $G_{i\xi} = G_{\xi i} = 0$, $G_{\xi\xi} = 1$, and by (A 28), we get for the inverse metric tensor $G^{i\xi} = G^{\xi i} = 0$, $G^{\xi\xi} = 1$. The pure tangential components of the thin film metric and its inverse can be expressed as a second-order surface tensor polynomial in $\xi \boldsymbol{B}$ and a second-order expansion

$$G_{ij} = g_{ij} - 2\xi B_{ij} + \xi^2 [\boldsymbol{B}^2]_{ij} \quad \text{and} \quad G^{ij} = g^{ij} + 2\xi B^{ij} + \mathcal{O}(\xi^2), \tag{3.3}$$

respectively. Consequently, there is no need for rescaling while lowering or rising the normal coordinate index ξ, i.e. for an arbitrary thin film tensor $\boldsymbol{W}$ it holds

$$W^{\cdots\xi\cdots}_{\cdots\cdots} = G^{\xi I} W^{\cdots\cdots}_{\cdots I\cdots} = W^{\cdots\cdots}_{\cdots\xi\cdots}. \tag{3.4}$$

Moreover, a contraction of two arbitrary thin film tensor $\boldsymbol{W}$ and $\tilde{\boldsymbol{W}}$ restricted to the surface results in a contraction of the tangential part w.r.t. the surface metric and a product of the normal part, i.e.

$$\begin{aligned} W^{\cdots\cdots}_{\cdots I\cdots} \tilde{W}^{\cdots I\cdots}_{\cdots\cdots}|_{\mathcal{S}} &= G^{IJ} W^{\cdots\cdots}_{\cdots I\cdots} \tilde{W}^{\cdots\cdots}_{\cdots J\cdots}|_{\mathcal{S}} = g^{ij} W^{\cdots\cdots}_{\cdots i\cdots} \tilde{W}^{\cdots\cdots}_{\cdots j\cdots}|_{\mathcal{S}} + W^{\cdots\cdots}_{\cdots\xi\cdots} \tilde{W}^{\cdots\cdots}_{\cdots\xi\cdots}|_{\mathcal{S}} \\ &= W^{\cdots\cdots}_{\cdots i\cdots} \tilde{W}^{\cdots i\cdots}_{\cdots\cdots}|_{\mathcal{S}} + W^{\cdots\cdots}_{\cdots\xi\cdots} \tilde{W}^{\cdots\cdots}_{\cdots\xi\cdots}|_{\mathcal{S}}. \end{aligned} \tag{3.5}$$

To deal with covariant derivatives, we have to take the Christoffel symbols into account. It is sufficient to expand $\mathbb{\Gamma}^K_{IJ}$ first order in normal direction, as we only use first-order derivatives and

[1]The suffix $\boldsymbol{g}$ will be omitted, if it is clear which metric the scalar product refers to.

no partial derivatives of the symbols are necessary. Hence, (3.3) result in

$$\mathbb{\Gamma}^k_{ij} = \Gamma^k_{ij} + \mathcal{O}(\xi), \quad \mathbb{\Gamma}^\xi_{ij} = B_{ij} + \mathcal{O}(\xi), \quad \mathbb{\Gamma}^K_{\xi\xi} = \mathbb{\Gamma}^\xi_{I\xi} = \mathbb{\Gamma}^\xi_{\xi I} = 0 \quad \text{and} \quad \mathbb{\Gamma}^k_{i\xi} = \mathbb{\Gamma}^k_{\xi i} = -B_{ij} + \mathcal{O}(\xi). \tag{3.6}$$

The volume element $\mathrm{d}V$ can be split up into a surface and a normal part by (A 36), i.e.

$$\mathrm{d}V = \sqrt{\det \boldsymbol{G}}\,\mathrm{d}u\,\mathrm{d}v\mathrm{d}\xi = (1 - \xi\mathcal{H} + \xi^2\mathcal{K})\sqrt{\det \boldsymbol{g}}\,\mathrm{d}u\,\mathrm{d}v\,\mathrm{d}\xi = (1 - \xi\mathcal{H} + \xi^2\mathcal{K})\,\mathrm{d}\mathcal{S}\,\mathrm{d}\xi. \tag{3.7}$$

We use a generalization of the tensor transpose operator T. This general transpose operator $T_\sigma : \mathrm{T}^{(n)}\mathcal{M} \to \mathrm{T}^{(n)}\mathcal{M}$ for n-tensors W on a Riemannian manifold $\mathcal{M}$ is defined w.r.t. a permutation $\sigma \in \mathrm{Sym}_n$ by

$$W^{T_\sigma}(v_1, \ldots, v_n) := W(v_{\sigma(1)}, \ldots, v_{\sigma(n)}), \tag{3.8}$$

for co- or contravariant vector fields $v_1, \ldots, v_n \in \mathrm{T}\mathcal{M}$, or $\mathrm{T}^*\mathcal{M}$, respectively. Hence, $T_{(1\,2)}$ is the ordinary transpose operator T for 2-tensors. The transpose T_σ is an operator on multilinear forms and does not depend on any choice of coordinates as a consequence. However, if a coordinate system is chosen, then T_σ is describable through σ-permuting the indices, e.g. for $W \in \mathrm{T}^2{}_1\mathcal{M}$, $\sigma = (2\,3)$ and indices $\alpha_1, \alpha_2, \alpha_3 \in \{1, \ldots, \dim(\mathcal{M})\}$, we obtain

$$\{W^{\alpha_1\alpha_2}{}_{\alpha_3}\}^{T_{(2\,3)}} = \{W^{\alpha_1}{}_{\alpha_3}{}^{\alpha_2}\}. \tag{3.9}$$

4. Thin film limit

Thin film limits require a reduction of degrees of freedom. We deal with this issue by setting Dirichlet boundary conditions for the normal parts of $\boldsymbol{Q}$ and postulate a priori a minimum of the free energy on the inner and outer boundary of the thin film. This is achieved by considering natural boundary condition of the weak Euler–Lagrange equation. In this setting, we restrict the density of $\mathcal{F}^{\mathcal{S}_h}$ to the surface and integrate in normal direction to obtain the surface energy $\mathcal{F}^{\mathcal{S}}$. In the same way, we also show the consistency of the thin film and surface L^2-gradient flows. The next subsection considers the reformulation of the surface Landau–de Gennes energy to obtain the formulation in (2.4), which allows a distinction of extrinsic and intrinsic contributions. Finally, we present a strong formulation of the derived equation of motion.

(i) Derivation of thin film limits

The free energy (2.2) in the thin film $\mathcal{S}_h$ in index notation reads

$$\left.\begin{aligned} \mathcal{F}^{\mathcal{S}_h}_{\mathrm{el}}[\boldsymbol{Q}] &= \frac{1}{2}\int_{\mathcal{S}_h} L_1 Q_{IJ;K}Q^{IJ;K} + L_2 Q_I{}^J{}_{;J}Q^{IK}{}_{;K} + L_3 Q_{IJ;K}Q^{IK;J} + L_6 Q^{KL}Q_{IJ;K}Q^{IJ}{}_{;L}\,\mathrm{d}V \\ \text{and} \quad \mathcal{F}^{\mathcal{S}_h}_{\mathrm{bulk}}[\boldsymbol{Q}] &= \int_{\mathcal{S}_h} aQ_{IJ}Q^{JI} + \frac{2}{3}bQ_{IJ}Q^{JK}Q_K{}^I + cQ_{IJ}Q^{JK}Q_{KL}Q^{LI}\,\mathrm{d}V. \end{aligned}\right\} \tag{4.1}$$

With respect to arbitrary thin film Q-tensors $\boldsymbol{\Psi} \in \mathcal{Q}(\mathcal{S}_h)$, the corresponding first variations are

$$\delta\mathcal{F}^{\mathcal{S}_h}_{\mathrm{el}}(\boldsymbol{Q}, \boldsymbol{\Psi}) = \int_{\mathcal{S}_h} \Psi_{IJ;K}(L_1 Q^{IJ;K} + L_3 Q^{IK;J} + L_6 Q^{KL}Q^{IJ}{}_{;L}) + L_2 \Psi_I{}^J{}_{;J}\,Q^{IK}{}_{;K} + \frac{L_6}{2}\Psi_{IJ}Q_{KL}{}^{;I}Q^{KL;J}\,\mathrm{d}V \tag{4.2}$$

and

$$\delta\mathcal{F}^{\mathcal{S}_h}_{\mathrm{bulk}}(\boldsymbol{Q}, \boldsymbol{\Psi}) = 2\int_{\mathcal{S}_h} ((a + cQ_{KL}Q^{KL})Q^{IJ} + bQ^{IK}Q^J_K)\Psi_{IJ}\,\mathrm{d}V. \tag{4.3}$$

To find local minimizers of the functional $\mathcal{F}^{\mathcal{S}_h} = \mathcal{F}^{\mathcal{S}_h}_{\mathrm{el}} + \mathcal{F}^{\mathcal{S}_h}_{\mathrm{bulk}}$, we are using the L^2-gradient flow

$$\int_{\mathcal{S}_h} \langle \partial_t \boldsymbol{Q}, \boldsymbol{\Psi}\rangle\,\mathrm{d}V = -\delta\mathcal{F}^{\mathcal{S}_h}(\boldsymbol{Q}, \boldsymbol{\Psi}) = -\int_{\mathcal{S}_h} \langle \nabla_{L^2}\mathcal{F}^{\mathcal{S}_h}, \boldsymbol{\Psi}\rangle\,\mathrm{d}V, \tag{4.4}$$

for all $\boldsymbol{\Psi} \in \mathcal{Q}(\mathcal{S}_h)$. However, integration by parts of (4.2) gives

$$\delta\mathcal{F}^{\mathcal{S}_h}(\boldsymbol{Q},\boldsymbol{\Psi}) = \int_{\mathcal{S}_h} \langle \nabla_{L2}\mathcal{F}^{\mathcal{S}_h}, \boldsymbol{\Psi}\rangle \,\mathrm{d}V + \int_{\partial\mathcal{S}_h} L_2 Q_I{}^J{}_{;J}\Psi^I_{\ \xi} + (L_1 Q_{IJ;\xi} + L_3 Q_{I\xi;J} + L_6 Q^{\xi K} Q_{IJ;K})\Psi^{IJ}\,\mathrm{d}A, \tag{4.5}$$

where $\mathrm{d}A$ is the volume form of the boundary surfaces. For the choice of essential boundary conditions, we require that $\boldsymbol{Q}$ has to have two eigenvectors in the boundary tangential bundle and the remaining eigenvector has to be the boundary normal, i.e. for $\boldsymbol{P} \in \mathrm{T}\partial\mathcal{S}_h$ a pure covariant representation of $\boldsymbol{Q}$ at the boundary is

$$\boldsymbol{Q} = S_1 \boldsymbol{P}^\flat \otimes \boldsymbol{P}^\flat + S_2 \boldsymbol{\nu}^\flat \otimes \boldsymbol{\nu}^\flat - \tfrac{1}{3}(S_1 + S_2)\boldsymbol{G} \tag{4.6}$$

with scalar order parameter S_1 and S_2. Hence, it holds $Q_{i\xi} = Q_{\xi i} = 0$ and $Q_{\xi\xi} = \frac{1}{3}(2S_2 - S_1)$. For simplicity, we set the pure normal part of $\boldsymbol{Q}$ constant, i.e. $Q_{\xi\xi} = \beta \in \mathbb{R}$ at $\partial\mathcal{S}_h$. Therefore, $\boldsymbol{\Psi}$ has to be in $\mathcal{Q}_0(\mathcal{S}_h) := \{\boldsymbol{\Psi} \in \mathcal{Q}(\mathcal{S}_h) : \Psi_{I\xi} = \Psi_{\xi I} = 0 \text{ at } \partial\mathcal{S}_h\}$, and we consider the natural boundary conditions $0 = (L_1 + L_6\beta)Q_{ij;\xi} + L_3 Q_{i\xi;j}$ at $\partial\mathcal{S}_h$, so that the boundary integral in (4.5) vanishes. Here, our analysis differs from previous results, which deal with a global determination of the normal derivatives in the whole bulk of $\mathcal{S}_h$ by parallel transport $\nabla_\xi \boldsymbol{Q} = 0$, or by $\partial_\xi \boldsymbol{Q} = 0$, see [21,22].

With lemma A.7, we can relate the anchoring conditions to surface identities

$$\left.\begin{aligned} &Q_{\xi\xi}|_{\mathcal{S}} = \beta + \mathcal{O}(h^2), \quad \partial_\xi Q_{\xi\xi}|_{\mathcal{S}} = \mathcal{O}(h^2), \quad (L_1 + L_6\beta)Q_{ij;\xi}|_{\mathcal{S}} + L_3 Q_{i\xi;j}|_{\mathcal{S}} = \mathcal{O}(h^2) \\ \text{and} \quad &Q_{i\xi}|_{\mathcal{S}} = Q_{\xi i}|_{\mathcal{S}} = \mathcal{O}(h^2) \quad \partial_\xi Q_{i\xi}|_{\mathcal{S}} = \partial_\xi Q_{\xi i}|_{\mathcal{S}} = \mathcal{O}(h^2). \end{aligned}\right\} \tag{4.7}$$

Evaluating $\boldsymbol{\Psi} \in \mathcal{Q}_0(\mathcal{S}_h)$ at the surface results in $\Psi_{I\xi}|_{\mathcal{S}} = \Psi_{\xi I}|_{\mathcal{S}} = \partial_\xi \Psi_{I\xi}|_{\mathcal{S}} = \partial_\xi \Psi_{\xi I}|_{\mathcal{S}} = \mathcal{O}(h^2)$. The restricted Q-tensor $\{Q_{ij}|_{\mathcal{S}}\} \in \mathrm{T}^{(2)}\mathcal{S}$ is not a Q-tensor, because $\mathrm{tr}_{\boldsymbol{g}}\{Q_{ij}|_{\mathcal{S}}\} = \mathrm{tr}_{\boldsymbol{G}}\boldsymbol{Q}|_{\mathcal{S}} - Q_{\xi\xi}|_{\mathcal{S}} = -Q_{\xi\xi}|_{\mathcal{S}}$. We thus project $\{Q_{ij}|_{\mathcal{S}}\}$ to $\mathcal{Q}(\mathcal{S})$ with the orthogonal projection

$$\mathrm{P}_{\mathcal{Q}} : \mathrm{T}^{(2)}\mathcal{S} \to \mathcal{Q}(\mathcal{S}), \quad \boldsymbol{t} \mapsto \tfrac{1}{2}(\boldsymbol{t} + \boldsymbol{t}^T - (\mathrm{tr}_{\boldsymbol{g}}\boldsymbol{t})\boldsymbol{g}) \tag{4.8}$$

and define $\boldsymbol{q} \in \mathcal{Q}(\mathcal{S})$ by

$$\boldsymbol{q} := \mathrm{P}_{\mathcal{Q}}\{Q_{ij}|_{\mathcal{S}}\} = \{Q_{ij}|_{\mathcal{S}}\} + \frac{\beta}{2}\boldsymbol{g} + \mathcal{O}(h^2). \tag{4.9}$$

For $\boldsymbol{\Psi} \in \mathcal{Q}_0(\mathcal{S}_h)$, the tangential part is already a Q-tensor up to $\mathcal{O}(h^2)$. Therefore, we define $\psi_{ij} := \Psi_{ij}|_{\mathcal{S}} + \frac{1}{2}\psi_{\xi\xi}|_{\mathcal{S}} g_{ij} = \Psi_{ij}|_{\mathcal{S}} + \mathcal{O}(h^2)$, where $\boldsymbol{\psi} \in \mathcal{Q}(\mathcal{S})$. With (3.1), (3.2), (3.6), (4.7), (4.9) and the tensor shift $\sigma_\omega(\boldsymbol{q}) := \boldsymbol{q} - (\omega/2)\beta\boldsymbol{g}$, we can determine all covariant derivatives restricted to the surface by

$$\left.\begin{aligned} &Q_{\xi\xi;\xi}|_{\mathcal{S}} = \partial_\xi Q_{\xi\xi}|_{\mathcal{S}} = \mathcal{O}(h^2), \\ &Q_{i\xi;\xi}|_{\mathcal{S}} = Q_{\xi i;\xi}|_{\mathcal{S}} = \partial_\xi Q_{i\xi}|_{\mathcal{S}} - \Gamma^K_{\xi i} Q_{K\xi}|_{\mathcal{S}} = \mathcal{O}(h^2), \\ &Q_{\xi\xi;k}|_{\mathcal{S}} = \partial_k Q_{\xi\xi}|_{\mathcal{S}} - 2\Gamma^L_{k\xi} Q_{L\xi}|_{\mathcal{S}} = \mathcal{O}(h^2), \\ &Q_{i\xi;k}|_{\mathcal{S}} = Q_{\xi i;k}|_{\mathcal{S}} = \partial_k Q_{i\xi}|_{\mathcal{S}} - \Gamma^l_{ki} Q_{l\xi}|_{\mathcal{S}} - \Gamma^\xi_{ki} Q_{\xi\xi}|_{\mathcal{S}} - \Gamma^l_{k\xi} Q_{il}|_{\mathcal{S}} \\ &\qquad = -\beta B_{ik} + (q_{il} - \frac{\beta}{2} g_{il})B^l{}_k + \mathcal{O}(h^2) = [\sigma_3(\boldsymbol{q})\boldsymbol{B}]_{ik} + \mathcal{O}(h^2), \\ &Q_{ij;\xi}|_{\mathcal{S}} = -\frac{L_3}{L_1 + L_6\beta} Q_{i\xi;j}|_{\mathcal{S}} + \mathcal{O}(h^2) = -\frac{L_3}{L_1 + L_6\beta}[\sigma_3(\boldsymbol{q})\boldsymbol{B}]_{ik} + \mathcal{O}(h^2) \\ \text{and} \quad &Q_{ij;k}|_{\mathcal{S}} = \partial_k Q_{ij}|_{\mathcal{S}} - \Gamma^l_{ki} Q_{lj}|_{\mathcal{S}} - \Gamma^\xi_{ki} Q_{\xi j}|_{\mathcal{S}} - \Gamma^l_{kj} Q_{il}|_{\mathcal{S}} - \Gamma^\xi_{kj} Q_{i\xi}|_{\mathcal{S}} \\ &\qquad = \partial_k Q_{ij}|_{\mathcal{S}} - \Gamma^l_{ki} Q_{lj}|_{\mathcal{S}} - \Gamma^l_{kj} Q_{il}|_{\mathcal{S}} + \mathcal{O}(h^2) = [\sigma_1(\boldsymbol{q})]_{ij|k} + \mathcal{O}(h^2) \\ &\qquad = q_{ij|k} + \mathcal{O}(h^2). \end{aligned}\right\} \tag{4.10}$$

Analogously, for the components of the covariant derivative $\nabla\boldsymbol{\Psi}|_{\mathcal{S}}$, we obtain $\Psi_{I\xi;\xi}|_{\mathcal{S}} = \Psi_{\xi I;\xi}|_{\mathcal{S}} = \Psi_{\xi\xi;I}|_{\mathcal{S}} = \mathcal{O}(h^2)$, $\Psi_{i\xi;k}|_{\mathcal{S}} = \Psi_{\xi i;k}|_{\mathcal{S}} = [\boldsymbol{\psi}\boldsymbol{B}]_{ik} + \mathcal{O}(h^2)$ and $\Psi_{ij;k}|_{\mathcal{S}} = \psi_{ij|k} + \mathcal{O}(h^2)$. Note, in the absence of natural boundary conditions for $\boldsymbol{\Psi}$, the covariant normal derivatives $\Psi_{ij;\xi}|_{\mathcal{S}}$ of the tangential components stay undetermined. However, as we will see, the thin film limit of the L^2-gradient

flow (4.4) does not depend on these derivatives. Adding up the three terms in (4.1) with factors L_1, L_3 and L_6, factoring $\nabla \boldsymbol{Q}$ out, restricting to the surface and considering (3.4) and (3.5), results in

$$\begin{aligned}
&L_1\|\nabla \boldsymbol{Q}\|_{\boldsymbol{G}}^2|_{\mathcal{S}} + L_3\langle \nabla \boldsymbol{Q}, (\nabla \boldsymbol{Q})^{T_{(23)}}\rangle_{\boldsymbol{G}}|_{\mathcal{S}} + L_6\langle (\nabla \boldsymbol{Q})\boldsymbol{Q}, \nabla \boldsymbol{Q}\rangle_{\boldsymbol{G}}|_{\mathcal{S}} \\
&\quad = Q_{IJ;K}(L_1 Q^{IJ;K} + L_3 Q^{IK;J} + L_6 Q^{KL} Q^{IJ}{}_{;L})|_{\mathcal{S}} \\
&\quad = Q_{ij;k}(L_1 Q^{ij;k} + L_3 Q^{ik;j} + L_6 Q^{kl} Q^{ij}{}_{;l})|_{\mathcal{S}} + Q_{\xi j;k}(L_1 Q^{\xi j;k} + L_3 Q^{\xi k;j} + L_6 Q^{kl} Q^{\xi j}{}_{;l})|_{\mathcal{S}} \\
&\qquad + Q_{i\xi;k}(L_1 Q^{i\xi;k} + L_3 Q^{ik;\xi} + L_6 Q^{kl} Q^{i\xi}{}_{;l})|_{\mathcal{S}} + Q_{ij;\xi}(L_1 Q^{ij;\xi} + L_3 Q^{i\xi;j} + L_6 Q^{\xi\xi} Q^{ij}{}_{;\xi})|_{\mathcal{S}} + \mathcal{O}(h^2) \\
&\quad = \left(L_1 - \frac{\beta}{2}L_6\right)\|\nabla \boldsymbol{q}\|_{\boldsymbol{g}}^2 + L_3\langle \nabla \boldsymbol{q}, (\nabla \boldsymbol{q})^{T_{(23)}}\rangle_{\boldsymbol{g}} + L_6\langle (\nabla \boldsymbol{q})\boldsymbol{q}, \nabla \boldsymbol{q}\rangle_{\boldsymbol{g}} + \left(2L_1 - \frac{L_3^2}{L_1 + L_6\beta}\right)\|\sigma_3(\boldsymbol{q})\boldsymbol{B}\|_{\boldsymbol{g}}^2 \\
&\qquad + L_3 \mathrm{tr}_{\boldsymbol{g}}(\sigma_3(\boldsymbol{q})\boldsymbol{B})^2 + 2L_6\langle \sigma_3(\boldsymbol{q})\boldsymbol{B}\sigma_1(\boldsymbol{q}), \sigma_3(\boldsymbol{q})\boldsymbol{B}\rangle_{\boldsymbol{g}} + \mathcal{O}(h^2). \qquad (4.11)
\end{aligned}$$

With $\mathrm{tr}\,\boldsymbol{q}^3 = 0$, we obtain for the remaining terms

$$\begin{aligned}
\|\mathrm{div}\boldsymbol{Q}\|_{\boldsymbol{G}}^2|_{\mathcal{S}} &= Q_I{}^J{}_{;J} Q^{IK}{}_{;K}|_{\mathcal{S}} = Q_i{}^j{}_{;j} Q^{ik}{}_{;k}|_{\mathcal{S}} + Q_\xi{}^j{}_{;j} Q_\xi{}^k{}_{;k}|_{\mathcal{S}} + \mathcal{O}(h^2) \\
&= \|\mathrm{div}\boldsymbol{q}\|_{\boldsymbol{g}}^2 + (\mathrm{tr}_{\boldsymbol{g}}(\sigma_3(\boldsymbol{q})\boldsymbol{B}))^2 + \mathcal{O}(h^2), \qquad (4.12) \\
\mathrm{tr}_{\boldsymbol{G}}\boldsymbol{Q}^2|_{\mathcal{S}} &= Q_{IJ}Q^{JI}|_{\mathcal{S}} = Q_{ij}Q^{ji}|_{\mathcal{S}} + (Q_{\xi\xi})^2|_{\mathcal{S}} + \mathcal{O}(h^2) \\
&= \mathrm{tr}_{\boldsymbol{g}}\left(\boldsymbol{q} - \frac{\beta}{2}\boldsymbol{g}\right)^2 + \beta^2 + \mathcal{O}(h^2) = \mathrm{tr}_{\boldsymbol{g}}\boldsymbol{q}^2 + \frac{3}{2}\beta^2 + \mathcal{O}(h^2), \qquad (4.13) \\
\mathrm{tr}_{\boldsymbol{G}}\boldsymbol{Q}^3|_{\mathcal{S}} &= Q_{IJ}Q^{JK}Q_K{}^I|_{\mathcal{S}} = Q_{ij}Q^{jk}Q_k{}^i|_{\mathcal{S}} + (Q_{\xi\xi})^3|_{\mathcal{S}} + \mathcal{O}(h^2) \\
&= \mathrm{tr}_{\boldsymbol{g}}\left(\boldsymbol{q} - \frac{\beta}{2}\boldsymbol{g}\right)^3 + \beta^3 + \mathcal{O}(h^2) = \frac{3}{2}\beta\left(\frac{\beta^2}{2} - \mathrm{tr}_{\boldsymbol{g}}\boldsymbol{q}^2\right) + \mathcal{O}(h^2) \qquad (4.14)
\end{aligned}$$

and

$$\mathrm{tr}_{\boldsymbol{G}}\boldsymbol{Q}^4|_{\mathcal{S}} = \frac{1}{2}(\mathrm{tr}_{\boldsymbol{G}}\boldsymbol{Q}^2 t)^2|_{\mathcal{S}} = \mathrm{tr}_{\boldsymbol{g}}\boldsymbol{q}^4 + \frac{3}{2}\beta^2\mathrm{tr}_{\boldsymbol{g}}\boldsymbol{q}^2 + \frac{9}{8}\beta^4 + \mathcal{O}(h^2). \qquad (4.15)$$

Adding all these up, we can define $\mathcal{F}^{\mathcal{S}} := \mathcal{F}^{\mathcal{S}}_{\mathrm{el}} + \mathcal{F}^{\mathcal{S}}_{\mathrm{bulk}}$ by

$$\left.\begin{aligned}
\mathcal{F}^{\mathcal{S}}_{\mathrm{el}}[\boldsymbol{q}] &:= \frac{1}{2}\int_{\mathcal{S}} \left(L_1 - \frac{\beta}{2}L_6\right)\|\nabla \boldsymbol{q}\|^2 + L_2\|\mathrm{div}\,\boldsymbol{q}\|^2 + L_3\langle \nabla \boldsymbol{q}, (\nabla \boldsymbol{q})^{T_{(23)}}\rangle \\
&\quad + L_6\langle (\nabla \boldsymbol{q})\boldsymbol{q}, \nabla \boldsymbol{q}\rangle + \left(2L_1 - \frac{L_3^2}{L_1 + L_6\beta}\right)\|\sigma_3(\boldsymbol{q})\boldsymbol{B}\|^2 + L_2(\mathrm{tr}(\sigma_3(\boldsymbol{q})\boldsymbol{B}))^2 \\
&\quad + L_3\mathrm{tr}(\sigma_3(\boldsymbol{q})\boldsymbol{B})^2 + 2L_6\langle \sigma_3(\boldsymbol{q})\boldsymbol{B}\sigma_1(\boldsymbol{q}), \sigma_3(\boldsymbol{q})\boldsymbol{B}\rangle\,\mathrm{d}\mathcal{S} \\
\text{and} \quad \mathcal{F}^{\mathcal{S}}_{\mathrm{bulk}}[\boldsymbol{q}] &:= \int_{\mathcal{S}} \frac{1}{2}(2a - 2b\beta + 3c\beta^2)\mathrm{tr}\,\boldsymbol{q}^2 + c\mathrm{tr}\,\boldsymbol{q}^4 + \frac{\beta^2}{8}(12a + 4b\beta + 9c\beta^2)\,\mathrm{d}\mathcal{S}
\end{aligned}\right\} \qquad (4.16)$$

and by the rectangle rule and (3.7), we obtain for $h \to 0$

$$\begin{aligned}
\frac{1}{h}\mathcal{F}^{\mathcal{S}_h} &= \frac{1}{h}\int_{\mathcal{S}_h} F^{\mathcal{S}_h}\,\mathrm{d}V = \frac{1}{h}\int_{-h/2}^{h/2}\int_{\mathcal{S}} (1 - \xi\mathcal{H} + \xi^2\mathcal{K})F^{\mathcal{S}_h}\,\mathrm{d}\mathcal{S}\,\mathrm{d}\xi = \int_{\mathcal{S}} F^{\mathcal{S}}\,\mathrm{d}\mathcal{S} + \mathcal{O}(h^2) \\
&= \mathcal{F}^{\mathcal{S}} + \mathcal{O}(h^2) \longrightarrow \mathcal{F}^{\mathcal{S}}. \qquad (4.17)
\end{aligned}$$

Consequently, the energies $\mathcal{F}^{\mathcal{S}}$ and $\mathcal{F}^{\mathcal{S}_h}$ are consistent w.r.t. the thickness h. To show a similar asymptotic behaviour for the L^2-gradient flows, we investigate the first variation $\delta\mathcal{F}^{\mathcal{S}_h} = \delta\mathcal{F}^{\mathcal{S}_h}_{\mathrm{el}} +$

$\delta\mathcal{F}^{\mathcal{S}_h}_{\text{bulk}}$ in (4.2) and compare with the first variation $\delta\mathcal{F}^{\mathcal{S}} = \delta\mathcal{F}^{\mathcal{S}}_{\text{el}} + \delta\mathcal{F}^{\mathcal{S}}_{\text{bulk}}$, where

$$\begin{aligned}\delta\mathcal{F}^{\mathcal{S}}_{\text{el}}(\boldsymbol{q},\boldsymbol{\psi}) = \int_{\mathcal{S}} &\left(L_1 - \frac{\beta}{2}L_6\right)\langle\nabla\boldsymbol{q},\nabla\boldsymbol{\psi}\rangle + L_2\langle\operatorname{div}\boldsymbol{q},\operatorname{div}\boldsymbol{\psi}\rangle + L_3\langle\nabla\boldsymbol{q},(\nabla\boldsymbol{\psi})^{T_{(23)}}\rangle\\ &+ L_6\left(\langle(\nabla\boldsymbol{q})\boldsymbol{q},\nabla\boldsymbol{\psi}\rangle + \frac{1}{2}\langle(\nabla\boldsymbol{q})\boldsymbol{\psi},\nabla\boldsymbol{q}\rangle\right) + \left(2L_1 - \frac{L_3^2}{L_1+L_6\beta}\right)\langle\sigma_3(\boldsymbol{q})\boldsymbol{B},\boldsymbol{\psi}\boldsymbol{B}\rangle\\ &+ L_2\langle\sigma_3(\boldsymbol{q}),\boldsymbol{B}\rangle\langle\boldsymbol{B},\boldsymbol{\psi}\rangle + L_3\langle\boldsymbol{B}\sigma_3(\boldsymbol{q}),\boldsymbol{\psi}\boldsymbol{B}\rangle\\ &+ L_6(2\langle\sigma_3(\boldsymbol{q})\boldsymbol{B}\sigma_1(\boldsymbol{q}),\boldsymbol{\psi}\boldsymbol{B}\rangle + \langle\boldsymbol{B}(\sigma_3(\boldsymbol{q}))^2,\boldsymbol{\psi}\boldsymbol{B}\rangle)\,\mathrm{d}\mathcal{S}\end{aligned} \tag{4.18}$$

and

$$\delta\mathcal{F}^{\mathcal{S}}_{\text{bulk}}(\boldsymbol{q},\boldsymbol{\psi}) = \int_{\mathcal{S}} (2a - 2b\beta + 3c\beta^2)\langle\boldsymbol{q},\boldsymbol{\psi}\rangle + 2c\,\operatorname{tr}\boldsymbol{q}^2\langle\boldsymbol{q},\boldsymbol{\psi}\rangle\,\mathrm{d}\mathcal{S}. \tag{4.19}$$

Proceeding as before, we restrict the terms under the integral of $\delta\mathcal{F}^{\mathcal{S}_h}$ in (4.2) to the surface. For $\delta\mathcal{F}^{\mathcal{S}_h}_{\text{el}}$, we obtain

$$\begin{aligned}&\Psi_{IJ;K}(L_1Q^{IJ;K} + L_3Q^{IK;J} + L_6Q^{KL}Q^{IJ}{}_{;L})|_{\mathcal{S}}\\ &\quad= \Psi_{ij;k}(L_1Q^{ij;k} + L_3Q^{ik;j} + L_6Q^{kl}Q^{ij}{}_{;l})|_{\mathcal{S}}\\ &\qquad+ \Psi_{i\xi;k}(2L_1Q^{i\xi;k} + L_3(Q^{ik;\xi} + Q^{k\xi;i}) + 2L_6Q^{kl}Q^{i\xi}{}_{;l})|_{\mathcal{S}} + \mathcal{O}(h^2)\\ &\quad= \psi_{ij|k}\left(\left(L_1 - \frac{\beta}{2}L_6\right)q^{ij|k} + L_3q^{ik|j} + L_6q^{kl}q^{ij}{}_{|l}\right)\\ &\qquad+ [\boldsymbol{\psi}\boldsymbol{B}]_{ik}\left(\left(2L_1 - \frac{L_3^2}{L_1+L_6\beta}\right)[\sigma_3(\boldsymbol{q})\boldsymbol{B}]^{ik} + L_3[\sigma_3(\boldsymbol{q})\boldsymbol{B}]^{ki}\right)\\ &\qquad+ 2L_6[\boldsymbol{\psi}\boldsymbol{B}]_{ik}[\sigma_3(\boldsymbol{q})\boldsymbol{B}\sigma_1(\boldsymbol{q})]^{ik} + \mathcal{O}(h^2),\end{aligned} \tag{4.20}$$

$$\Psi_I{}^J{}_{;J}\,Q^{IK}{}_{;K}|_{\mathcal{S}} = \psi_i{}^j{}_{|j}q^{ik}{}_{|k} + [\boldsymbol{\psi}\boldsymbol{B}]^j{}_j[\sigma_3(\boldsymbol{q})\boldsymbol{B}]^k{}_k + \mathcal{O}(h^2) \tag{4.21}$$

and

$$\begin{aligned}\tfrac{1}{2}\Psi_{IJ}Q_{KL}{}^{;I}Q^{KL;J}|_{\mathcal{S}} &= \tfrac{1}{2}\Psi_{ij}(Q_{kl}{}^{;i}Q^{kl;j} + 2Q_{k\xi}{}^{;i}Q^{k\xi;j})|_{\mathcal{S}} + \mathcal{O}(h^2)\\ &= \tfrac{1}{2}\psi_{ij}q_{kl}{}^{|i}q^{kl|j} + \psi_{ij}[\boldsymbol{B}(\sigma_3(\boldsymbol{q}))^2\boldsymbol{B}]^{ij} + \mathcal{O}(h^2)\end{aligned} \tag{4.22}$$

and for $\delta\mathcal{F}^{\mathcal{S}_h}_{\text{bulk}}$

$$\begin{aligned}2(a + cQ_{KL}Q^{KL})Q^{IJ}\Psi_{IJ}|_{\mathcal{S}} &= (2a + 2cq_{kl}q^{kl} + 3c\beta^2)\left(q^{ij}\psi_{ij} - \frac{\beta}{2}\psi^i{}_i\right) + \mathcal{O}(h^2)\\ &= (2a + 3c\beta^2)\langle\boldsymbol{q},\boldsymbol{\psi}\rangle + 2c\operatorname{tr}\boldsymbol{q}^2\langle\boldsymbol{q},\boldsymbol{\psi}\rangle + \mathcal{O}(h^2)\end{aligned} \tag{4.23}$$

and

$$\begin{aligned}2bQ^{IK}Q_K{}^J\Psi_{IJ}|_{\mathcal{S}} &= 2bQ^{ik}Q_k{}^j\psi_{ij}|_{\mathcal{S}} + \mathcal{O}(h^2) = 2b\left([\boldsymbol{q}^2]^{ij} - \beta q^{ij} + \frac{\beta^2}{4}g^{ij}\right)\psi_{ij} + \mathcal{O}(h^2)\\ &= -2b\beta q^{ij}\psi_{ij} + b\left(\operatorname{tr}\boldsymbol{q}^2 + \frac{\beta^2}{2}\right)\psi^i{}_i + \mathcal{O}(h^2)\\ &= -2b\beta\langle\boldsymbol{q},\boldsymbol{\psi}\rangle + \mathcal{O}(h^2).\end{aligned} \tag{4.24}$$

where we used corollary A.4, i.e. $2\boldsymbol{q}^2 = (\operatorname{tr}\boldsymbol{q}^2)\boldsymbol{g}$, particularly. In summary, we see that $\langle\nabla_{L^2}\mathcal{F}^{\mathcal{S}_h},\boldsymbol{\Psi}\rangle|_{\mathcal{S}} = \langle\nabla_{L^2}\mathcal{F}^{\mathcal{S}},\boldsymbol{\psi}\rangle + \mathcal{O}(h^2)$ is valid. Moreover, as $\partial_t\boldsymbol{g} = 0$ for a stationary surface, we obtain $[\partial_t\boldsymbol{Q}|_{\mathcal{S}}]_{ij} = [\partial_t\boldsymbol{q}]_{ij} + \mathcal{O}(h^2)$. Finally, as in (4.17), we argue with the rectangle rule in normal direction and observe

$$\frac{1}{h}\int_{\mathcal{S}_h}\langle\nabla_{L2}\mathcal{F}^{\mathcal{S}_h} + \partial_t\boldsymbol{Q},\boldsymbol{\Psi}\rangle\,\mathrm{d}V = \int_{\mathcal{S}}\langle\nabla_{L^2}\mathcal{F}^{\mathcal{S}} + \partial_t\boldsymbol{q},\boldsymbol{\psi}\rangle\,\mathrm{d}\mathcal{S} + \mathcal{O}(h^2). \tag{4.25}$$

(ii) Surface energy

To have a better distinction between extrinsic terms, i.e. $\langle \boldsymbol{B}, \boldsymbol{q}\rangle$, and terms depending only on scalar curvatures $\mathcal{H}$ and $\mathcal{K}$ in the surface energy (4.16), we use corollary A.4 and obtain the substitutions

$$(\mathrm{tr}(\sigma_3(\boldsymbol{q})\boldsymbol{B}))^2 = \langle \boldsymbol{B}, \boldsymbol{q}\rangle^2 - 3\beta\mathcal{H}\langle \boldsymbol{B}, \boldsymbol{q}\rangle + \tfrac{9}{4}\beta^2\mathcal{H}^2, \tag{4.26}$$

$$\mathrm{tr}(\sigma_3(\boldsymbol{q})\boldsymbol{B})^2 = \langle \boldsymbol{B}, \boldsymbol{q}\rangle^2 + \mathcal{K}\mathrm{tr}\,\boldsymbol{q}^2 - 3\beta\mathcal{H}\langle \boldsymbol{B}, \boldsymbol{q}\rangle + \tfrac{9}{4}\beta^2(\mathcal{H}^2 - 2\mathcal{K}), \tag{4.27}$$

$$\|\sigma_3(\boldsymbol{q})\boldsymbol{B}\|^2 = \tfrac{1}{2}(\mathcal{H}^2 - 2\mathcal{K})\mathrm{tr}\,\boldsymbol{q}^2 - 3\beta\mathcal{H}\langle \boldsymbol{B}, \boldsymbol{q}\rangle + \tfrac{9}{4}\beta^2(\mathcal{H}^2 - 2\mathcal{K}) \tag{4.28}$$

and

$$\begin{aligned}\langle \sigma_3(\boldsymbol{q})\boldsymbol{B}\sigma_1(\boldsymbol{q}), \sigma_3(\boldsymbol{q})\boldsymbol{B}\rangle &= \tfrac{1}{2}\mathcal{H}\,\mathrm{tr}\,\boldsymbol{q}^2\langle \boldsymbol{B}, \boldsymbol{q}\rangle - \beta(3\langle \boldsymbol{B}, \boldsymbol{q}\rangle^2 + \tfrac{1}{4}(\mathcal{H}^2 + 10\mathcal{K}))\mathrm{tr}\,\boldsymbol{q}^2 \\ &\quad + \tfrac{15}{4}\mathcal{H}\beta^2\langle \boldsymbol{B}, \boldsymbol{q}\rangle - \tfrac{9}{8}\beta^3(\mathcal{H}^2 - 2\mathcal{K}),\end{aligned} \tag{4.29}$$

at the surface $\mathcal{S}$. Terms with invariant measurement of the gradient $\nabla\boldsymbol{q}$ differ only in zero-order quantities for a closed surface, see lemma A.1. Adding all these up, we obtain (2.4) and therefore in index notation

$$\left.\begin{aligned}\mathcal{F}^{\mathcal{S}}_{\mathrm{el}}[\boldsymbol{q}] &= \frac{1}{2}\int_{\mathcal{S}} L_1' q_{ij|k}q^{ij|k} + L_6 q^{kl}q_{ij|k}q^{ij}{}_{|l} + M_1 q_{ij}q^{ij} + M_2 B^{ij}B^{kl}q_{ij}q_{kl} \\ &\quad + M_3 B^{ij}q_{ij}q^{kl}q_{kl} + M_4 B^{ij}q_{ij} + C_0\,\mathrm{d}\mathcal{S} \\ \text{and}\qquad \mathcal{F}^{\mathcal{S}}_{\mathrm{bulk}}[\boldsymbol{q}] &:= \int_{\mathcal{S}} a' q_{ij}q^{ij} + c q_{ij}q^{jk}q_{kl}q^{li} + C_1\,\mathrm{d}\mathcal{S},\end{aligned}\right\} \tag{4.30}$$

with coefficient functions

$$\left.\begin{aligned}L_1' &:= L_1 + \frac{1}{2}(L_2 + L_3 - L_6\beta), \\ M_2 &:= L_2 + L_3 - 6L_6\beta, \\ M_3 &:= L_6\mathcal{H}, \\ M_1 &:= \frac{1}{2}\left(-L_6(\mathcal{H}^2 + 10\mathcal{K})\beta + \left(2L_1 - \frac{L_3^2}{L_1 + L_6\beta}\right)(\mathcal{H}^2 - 2\mathcal{K}) + (L_2 + L_3)\mathcal{K}\right), \\ M_4 &:= -3\left(2L_1 + L_2 + L_3 - \frac{5}{2}L_6\beta - \frac{L_3^2}{L_1 + L_6\beta}\right)\beta\mathcal{H}, \\ C_0 &:= \frac{9}{4}\left(\left(2L_1 + L_3 - L_6\beta - \frac{L_3^2}{L_1 + L_6\beta}\right)(\mathcal{H}^2 - 2\mathcal{K}) + L_2\mathcal{H}^2\right)\beta^2, \\ a' &:= \frac{1}{2}(2a - 2b\beta + 3c\beta^2) \\ \text{and}\qquad C_1 &:= \frac{\beta^2}{8}(12a + 4b\beta + 9c\beta^2).\end{aligned}\right\} \tag{4.31}$$

(iii) Surface equation of motion

To obtain the strong form of the surface L^2-gradient flow $\partial_t\boldsymbol{q} = -\nabla_{L^2}\mathcal{F}^{\mathcal{S}}$, we have to ensure

$$\int_{\mathcal{S}}\langle \partial_t\boldsymbol{q}, \boldsymbol{\psi}\rangle\,\mathrm{d}\mathcal{S} = -\int_{\mathcal{S}}\langle \nabla_{L^2}\mathcal{F}^{\mathcal{S}}, \boldsymbol{\psi}\rangle\,\mathrm{d}\mathcal{S}, \quad \forall\,\boldsymbol{\psi}\in\mathcal{Q}(\mathcal{S}), \tag{4.32}$$

w.r.t. the L^2 inner product over the space of Q-tensors and thus $\nabla_{L^2}\mathcal{F}^{\mathcal{S}} \in \mathcal{Q}(\mathcal{S})$. While for the first variations δ w.r.t. $\boldsymbol{q}$ in direction ψ

$$\frac{1}{2}\delta\int_{\mathcal{S}}\|\nabla\boldsymbol{q}\|^2\,\mathrm{d}\mathcal{S}=\int_{\mathcal{S}}\langle-\operatorname{div}\nabla\boldsymbol{q},\boldsymbol{\psi}\rangle\,\mathrm{d}\mathcal{S}, \tag{4.33}$$

$$\frac{1}{2}\delta\int_{\mathcal{S}}\operatorname{tr}\boldsymbol{q}^2\,\mathrm{d}\mathcal{S}=\int_{\mathcal{S}}\langle\boldsymbol{q},\boldsymbol{\psi}\rangle\,\mathrm{d}\mathcal{S} \tag{4.34}$$

and

$$\frac{1}{2}\delta\int_{\mathcal{S}}\operatorname{tr}\boldsymbol{q}^4\,\mathrm{d}\mathcal{S}=\int_{\mathcal{S}}\langle(\operatorname{tr}\boldsymbol{q}^2)\boldsymbol{q},\boldsymbol{\psi}\rangle\,\mathrm{d}\mathcal{S}, \tag{4.35}$$

the left argument of the inner product is already in $\mathcal{Q}(\mathcal{S})$, we have to apply $\mathrm{P}_{\mathcal{Q}}$ defined in (4.8) for the remaining terms, i.e.

$$\begin{aligned}\frac{1}{2}\delta\int_{\mathcal{S}}\langle(\nabla\boldsymbol{q})\boldsymbol{q},\nabla\boldsymbol{q}\rangle\,\mathrm{d}\mathcal{S}&=\int_{\mathcal{S}}\left(-(q_{ij|k}q^{kl})_{|l}+\frac{1}{2}q_{kl|i}q^{kl}{}_{|j}\right)\psi^{ij}\,\mathrm{d}\mathcal{S}\\&=\int_{\mathcal{S}}\left(-q_{ij|k|l}q^{kl}-q_{ij|k}q^{kl}{}_{|l}+\frac{1}{2}[\mathrm{P}_{\mathcal{Q}}\{q_{kl|i}q^{kl}{}_{|j}\}]_{ij}\right)\psi^{ij}\,\mathrm{d}\mathcal{S}\\&=\int_{\mathcal{S}}\left(-q_{ij|k|l}q^{kl}-q_{ij|k}q^{kl}{}_{|l}+\frac{1}{2}q_{kl|i}q^{kl}{}_{|j}-\frac{1}{4}q_{kl|m}q^{kl|m}g_{ij}\right)\psi^{ij}\,\mathrm{d}\mathcal{S}\\&=\int_{\mathcal{S}}\left\langle(-\nabla\nabla\boldsymbol{q}):\boldsymbol{q}-(\nabla\boldsymbol{q})\cdot\operatorname{div}\boldsymbol{q}+\frac{1}{2}(\nabla\boldsymbol{q})^{T_{(13)}}:\nabla\boldsymbol{q}-\frac{1}{4}\|\nabla\boldsymbol{q}\|^2\boldsymbol{g},\boldsymbol{\psi}\right\rangle\mathrm{d}\mathcal{S},\end{aligned} \tag{4.36}$$

$$\begin{aligned}\frac{1}{2}\delta\int_{\mathcal{S}}\langle\boldsymbol{B},\boldsymbol{q}\rangle^2\,\mathrm{d}\mathcal{S}&=\int_{\mathcal{S}}\langle\langle\boldsymbol{B},\boldsymbol{q}\rangle\boldsymbol{B},\boldsymbol{\psi}\rangle\,\mathrm{d}\mathcal{S}=\int_{\mathcal{S}}\langle\langle\boldsymbol{B},\boldsymbol{q}\rangle\mathrm{P}_{\mathcal{Q}}\boldsymbol{B},\boldsymbol{\psi}\rangle\,\mathrm{d}\mathcal{S}\\&=\int_{\mathcal{S}}\left\langle\langle\boldsymbol{B},\boldsymbol{q}\rangle\left(\boldsymbol{B}-\frac{1}{2}\mathcal{H}\boldsymbol{g}\right),\boldsymbol{\psi}\right\rangle\mathrm{d}\mathcal{S},\end{aligned} \tag{4.37}$$

$$\begin{aligned}\frac{1}{2}\delta\int_{\mathcal{S}}\operatorname{tr}\boldsymbol{q}^2\langle\boldsymbol{B},\boldsymbol{q}\rangle\,\mathrm{d}\mathcal{S}&=\int_{\mathcal{S}}\left\langle\frac{1}{2}\operatorname{tr}\boldsymbol{q}^2\boldsymbol{B}+\langle\boldsymbol{B},\boldsymbol{q}\rangle\boldsymbol{q},\boldsymbol{\psi}\right\rangle\mathrm{d}\mathcal{S}=\int_{\mathcal{S}}\left\langle\frac{1}{2}\operatorname{tr}\boldsymbol{q}^2\mathrm{P}_{\mathcal{Q}}\boldsymbol{B}+\langle\boldsymbol{B},\boldsymbol{q}\rangle\boldsymbol{q},\boldsymbol{\psi}\right\rangle\mathrm{d}\mathcal{S}\\&=\int_{\mathcal{S}}\left\langle\frac{1}{2}\operatorname{tr}\boldsymbol{q}^2\left(\boldsymbol{B}-\frac{1}{2}\mathcal{H}\boldsymbol{g}\right)+\langle\boldsymbol{B},\boldsymbol{q}\rangle\boldsymbol{q},\boldsymbol{\psi}\right\rangle\mathrm{d}\mathcal{S}\end{aligned} \tag{4.38}$$

and

$$\begin{aligned}\frac{1}{2}\delta\int_{\mathcal{S}}\langle\boldsymbol{B},\boldsymbol{q}\rangle\,\mathrm{d}\mathcal{S}&=\int_{\mathcal{S}}\left\langle\frac{1}{2}\boldsymbol{B},\boldsymbol{\psi}\right\rangle\mathrm{d}\mathcal{S}=\int_{\mathcal{S}}\left\langle\frac{1}{2}\mathrm{P}_{\mathcal{Q}}\boldsymbol{B},\boldsymbol{\psi}\right\rangle\mathrm{d}\mathcal{S}\\&=\int_{\mathcal{S}}\left\langle\frac{1}{2}\left(\boldsymbol{B}-\frac{1}{2}\mathcal{H}\boldsymbol{g}\right),\boldsymbol{\psi}\right\rangle\mathrm{d}\mathcal{S}.\end{aligned} \tag{4.39}$$

Finally, with $[\Delta^{dG}\boldsymbol{q}]_{ij}:=q_{ij}{}^{|k}{}_{|k}$, the div-Grad (Bochner) Laplace operator, we get the equation of motion (2.5), which reads in index notation

$$\begin{aligned}\partial_t q_{ij}=&L_1'q_{ij}{}^{|k}{}_{|k}+L_6\left(-q_{ij|k|l}q^{kl}-q_{ij|k}q^{kl}{}_{|l}+\frac{1}{2}q_{kl|i}q^{kl}{}_{|j}-\frac{1}{4}q_{kl|m}q^{kl|m}g_{ij}\right)\\&-(M_1+M_3B_{kl}q^{kl}+2a'+2cq_{kl}q^{kl})q_{ij}\\&-\left(M_2B_{kl}q^{kl}+\frac{M_3}{2}q_{kl}q^{kl}+\frac{M_4}{2}\right)\left(B_{ij}-\frac{1}{2}\mathcal{H}g_{ij}\right).\end{aligned} \tag{4.40}$$

After establishing weak consistences for the energies and the L^2-gradient flows in the thin film and at the surface in (4.17) and (4.25), we also have pointwise consistence for the evolution equation in the Q-tensor space restricted to the surface for sufficient regularity, i.e.

$$\|\mathrm{P}_{\mathcal{Q}}[\Pi(\partial_t\boldsymbol{Q}+\nabla_{L^2}\mathcal{F}^{\mathcal{S}_h}[\boldsymbol{Q}])|_{\mathcal{S}}\Pi]-(\partial_t\boldsymbol{q}+\nabla_{L^2}\mathcal{F}^{\mathcal{S}}[\boldsymbol{q}])\|_g=\mathcal{O}(h^2), \tag{4.41}$$

w.r.t. boundary conditions for $\boldsymbol{Q}$ at $\partial\mathcal{S}_h$ and initial condition $\boldsymbol{q}|_{t=0}=\Pi\boldsymbol{Q}|_{(\mathcal{S},t=0)}\Pi+\boldsymbol{\nu}\boldsymbol{Q}|_{(\mathcal{S},t=0)}\boldsymbol{\nu}$. This means, the order of performing the limit $h\to 0$ and formulating the local dynamic equation,

w.r.t. ∇_{L^2} flow, does not matter, i.e. the diagram

$$\left.\begin{array}{ccc} \mathcal{F}^{\mathcal{S}_h} & \xrightarrow[\frac{1}{h}]{h\to 0} & \mathcal{F}^{\mathcal{S}} \\ \nabla_{L^2}\text{flow}\downarrow & & \downarrow\nabla_{L^2}\text{flow} \\ \partial_t \boldsymbol{Q} = -\nabla_{L^2}\mathcal{F}^{\mathcal{S}_h}[\boldsymbol{Q}] & \xrightarrow[\mathrm{P}_{\mathcal{Q}},\,\Pi]{h\to 0} & \partial_t \boldsymbol{q} = -\nabla_{L^2}\mathcal{F}^{\mathcal{S}}[\boldsymbol{q}] \end{array}\right\} \tag{4.42}$$

commutes.

5. Discussion

We now discuss similarities and differences between the thin film and surface Landau–de Gennes energy and their physical implication. Besides the terms containing the extrinsic quantity $\boldsymbol{B}$ and its scalar-valued invariants, the surface Q-tensor energy (2.4) is similar to the thin film Q-tensor energy (2.2). While we have three scalar invariants for the gradient $\nabla_{\boldsymbol{G}}\boldsymbol{Q}$ in the thin film controlled by L_1, L_2 and L_3, at the surface we need only one for $\nabla_{\boldsymbol{g}}\boldsymbol{q}$ to formulate the distortion of $\boldsymbol{q}$, see lemma A.1. This behaviour seems to be a consequence of reducing the degree of freedoms of Q-tensors. Particularly, $\mathcal{Q}(\mathcal{S}_h)$ is a five-dimensional function-vector space, while $\mathcal{Q}(\mathcal{S})$ is only a two-dimensional function-vector space with improper rotation endomorphisms in the tangential bundle as basis tensors. Moreover, at the surface, we only consider the trace of even powers of $\boldsymbol{q}$ for the bulk energy as for $r \geq 0$ it holds

$$\operatorname{tr}\boldsymbol{q}^{2(r+1)} = \langle(\boldsymbol{q}^2)^{r+1}, \boldsymbol{g}\rangle = 2^{-(r+1)}(\operatorname{tr}\boldsymbol{q}^2)^{r+1}\|\boldsymbol{g}\|^2 = 2^{-r}(\operatorname{tr}\boldsymbol{q}^2)^{r+1} \tag{5.1}$$

and

$$\operatorname{tr}\boldsymbol{q}^{2r+1} = \langle(\boldsymbol{q}^2)^r, \boldsymbol{q}\rangle = 2^{-r}(\operatorname{tr}\boldsymbol{q}^2)^r\operatorname{tr}\boldsymbol{q} = 0, \tag{5.2}$$

see corollary A.4. This has several consequences. In principle, it leads to a change in phase transition type, as coexistence between a nematic and an isotropic phase is not possible without the $\operatorname{tr}\boldsymbol{q}^3$ term. However, as we will see, our model still allows coexistence. We first show that we can preserve the phase diagram of the thin film bulk energy. To limit complexity, we have considered $\boldsymbol{\nu}\boldsymbol{Q}\boldsymbol{\nu} = \beta$ to be constant. Similar assumptions have been made in [20,21]. Our approach chooses β such that surface and thin film formulation of bulk energy match. For $\beta = -\frac{1}{3}S^*$, where $S^* = (1/4c)(-b + \sqrt{b^2 - 24ac})$ indeed the minima of $\mathcal{F}^{\mathcal{S}_h}_{\text{bulk}}$ and $\mathcal{F}^{\mathcal{S}}_{\text{bulk}}$ are equal and are achieved for $S = S^*$, with $S = S_1 = S_2$ or $S = S_1$ if $S_2 = 0$ or $S = S_2$ if $S_1 = 0$. The reconstructed thin film Q-tensor $\boldsymbol{Q} = \boldsymbol{q} - (\beta/2)\Pi + \beta\boldsymbol{\nu}\otimes\boldsymbol{\nu}$ is uniaxial with eigenvalues $[\frac{2}{3}S, -\frac{1}{3}S, -\frac{1}{3}S]$. Figure 2 shows the phase diagram. Contrary to the modelling via degenerate states with $\beta = 0$ (e.g. [20]) the phase diagram of the bulk energy is preserved for $\beta = -\frac{1}{3}S^*$.

With the emergence of defects, the assumption $\beta = \text{const}$ becomes questionable and a more precise modelling would require to treat β as a degree of freedom. However, this would lead to an excessive amount of additional coupling terms in the elastic energy and thus makes the complexity of the model infeasible. A detailed derivation and interpretation of the additional terms thus remains an open question.

Considering the elastic energy, the surface model provides a set of new terms consisting of combinations of $\operatorname{tr}\boldsymbol{q}^2$ and $\langle\boldsymbol{B},\boldsymbol{q}\rangle$. These terms interact with the double-well potential $a'\operatorname{tr}\boldsymbol{q}^2 + c\operatorname{tr}\boldsymbol{q}^4$ of the surface bulk energy. By this interaction, the bulk potential can be deformed locally, as e.g. $M_1\operatorname{tr}\boldsymbol{q}^2$, depends on geometric properties $M_1 = M_1(\mathcal{H},\mathcal{K})$. So, while the bulk potential itself inhibits isotropic-nematic phase coexistence, a global phase coexistence can emerge on surfaces by local variance of geometric properties (figure 3).

The term $\langle\boldsymbol{B},\boldsymbol{q}\rangle$ imposes restrictions on energetic favourable ordering. This term can be expressed in terms of principal director $\boldsymbol{P}$ of $\boldsymbol{q}$ by $\langle\boldsymbol{B},\boldsymbol{q}\rangle = \boldsymbol{P}\boldsymbol{B}\boldsymbol{P} - \frac{1}{2}\mathcal{H}\|\boldsymbol{P}\|$ illustrating a geometric forcing towards the ordering along lines of minimal curvature. Such forcing does eliminate the rotational invariance of the four $+\frac{1}{2}$ defect configuration on an ellipsoid as demonstrated in

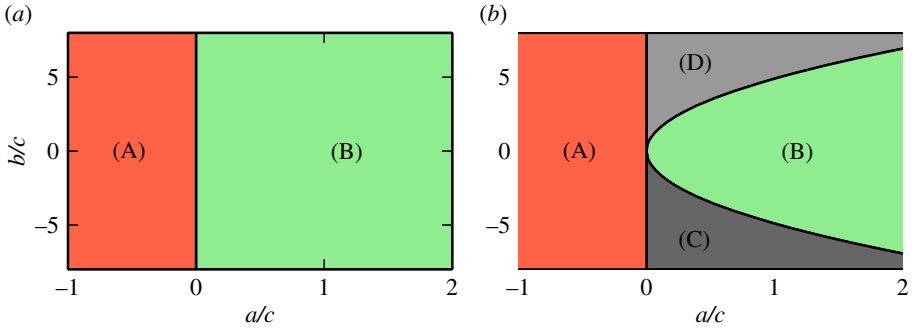

Figure 2. Phase diagram of bulk energy versus choice of β. (*a*) Double-well potential phase diagram for $\beta = 0$ exhibiting two domains enabling the existence of (A): stable nematic ordering $S^* \neq 0$ or (B): stable isotropic ordering $S^* = 0$. (*b*) Phase diagram for $\beta = -\frac{1}{3}S^*$ enabling additional stable phases discriminating between (C): only tangential nematic ordering is stable, $S^* > 0$ or (D): only normal nematic ordering is stable, $S^* < 0$. As we are interested only in tangential anchoring, (D) is not within the scope of this paper. (Online version in colour.)

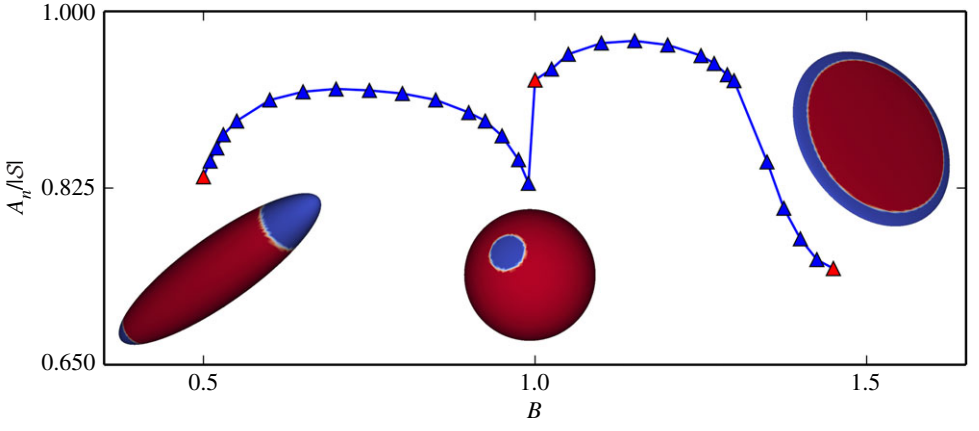

Figure 3. Curvature controls isotropic-nematic phase coexistence. Relative area of the nematic phase $A_n/|\mathcal{S}|$ as a function of the geometry of the ellipsoid, parametrized by its axis B. For prolates ($B < 1.0$), the isotropic phases are located at the high curvature regions at the poles. They increase with increasing curvature for $B \lesssim 0.6$. For oblates ($B > 1.0$), the isotropic phase is located at the high curvature region along the rim. It increases with increasing curvature for $B \gtrsim 1.2$. The non-monotone behaviour in between results from a rearrangement of two regions on a prolate to four regions on an oblate, which merge for larger B. The inlets show realizations with red (light grey) corresponding to the nematic and blue (dark grey) to the isotropic phase. The corresponding shape parameters are highlighted with red (light grey) triangle markers. To distinguish between both phases, a threshold of 10% of the expected norm of $\boldsymbol{q}$ is used. The model parameters are the same as in figure 1, except $\omega = 2.5$ to highlight the behaviour already for moderate curvatures. (Online version in colour.)

figure 4. The same effect has also been observed in surface Frank–Oseen model for surface polar liquid crystals [30].

Combining these effects provides a wide range of intriguing mechanisms coupling geometry and ordering with significant impacts on minimum energy states and dynamics. A more detailed elaboration of these interactions as well as a detailed description of the used numerical approach will be given elsewhere.

As a complementary result, we point out that the surface model for degenerate states in [20] can be reproduced by our model by choosing $\beta = 0$, $k = L_1 = (1/\sqrt{2})L_2 = -(1/\sqrt{2})L_3$, $k_{24} = -\sqrt{2}k$ and defining $2a = A$, $2c = C$. A one-to-one comparison with the models derived in [21–23] is more

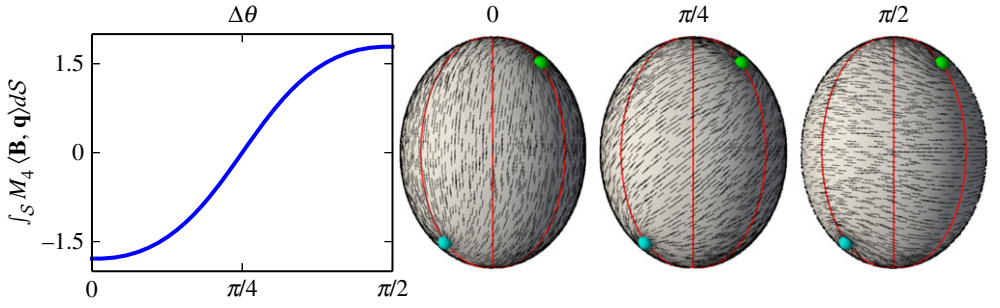

Figure 4. $\langle \boldsymbol{B}, \boldsymbol{q} \rangle$ term removes rotational invariance of elastic energy: (from left to right) elastic energy contribution of $\int_S M_4 \langle \boldsymbol{B}, \boldsymbol{q} \rangle \mathrm{d}\mathcal{S}$ under rotation $\triangle\theta$ of Q-tensor field $\boldsymbol{q}$. Energetic minimum at $\triangle\theta = 0$ with director parallel to lines of minimal curvature (marked in red), increased energy at intermediate state at $\triangle\theta = \pi/4$ and maximal energy for director orthogonal to lines of minimal curvature at $\triangle\theta = \pi/2$. Energy contributions of L_1' and M_1 are invariant under rotation and therefore constant. The model parameters are the same as in figure 1. (Online version in colour.)

complicated, as in contrast to our approach, which only uses the Levi–Civita connections ∇, other surface derivatives are introduced in [21–23], which make these models depending on the chosen coordinate system. A detailed comparison of numerical simulations might allow to point out similarities and differences.

At the end, we would like to come back to the raised issues concerning the third order L_6 term in (2.2). Owing to the unboundedness of the energy, which cannot be compensated by a polynomial bulk energy, the equation $\partial_t \boldsymbol{Q} = -\nabla_{L^2} \mathcal{F}^{\mathcal{S}_h}[\boldsymbol{Q}]$ is ill-posed [29]. However, it remains open if this result also holds for $\partial_t \boldsymbol{q} = -\nabla_{L^2} \mathcal{F}^{\mathcal{S}}[\boldsymbol{q}]$. In [37], it is shown that, under convenient choice of parameters, boundary conditions and initial conditions, the L^2-gradient flow does not diverge in a flat two-dimensional setting. We are confident, that this result is generalizable to curved surfaces and hence also for a thin shell, if h is sufficiently small. If this is not possible, the energy (2.2) should be modified. One possibility is to include fourth-order terms. A fully general theory of elastic energies, with a minimal set of $SO(3)$-invariant terms up to order four, is developed in [28]. This approach will alter the derived thin film limit and lead to additional terms that can be derived in a straightforward manner. But, it is also possible to replace the bulk energy in (2.2) by a singular potential, so that the entire energy is bounded from below (e.g. [29]). Note that, if such a bulk potential does not contain any derivatives affecting the natural anchoring condition in the variation, like the one used in [29], the thin film limit for the elastic part remains and thus, at least qualitatively, all our results also hold. We leave these analytical questions for future work and, to be on the safe side, restrict our numerical investigations to the case $L_6 = 0$.

6. Conclusion

We have asymptotically derived a surface Q-tensor model by performing the thin film limit. Instead of making assumptions on the Q-tensor field in the thin film we have prescribed a set of boundary conditions for the thin film. By requiring the normal components of $\boldsymbol{Q}$ to be compatible with the minimum of the bulk energy we were able to transfer main features of the thin film model, like uniaxiality or parameter-phase space, to the surface model. Nonetheless, these features break down in areas of defects. It still remains an open question how to treat defect areas properly in surface Q-tensor models.

The proposed approach to derive thin film limits is general and can also be used for other tensorial problems, e.g. in elasticity. Note that for deriving thin film limits containing higher-order derivatives, also higher-order expansions for thin film metric quantities are needed, e.g. $\mathbb{I}^k_{ij} = \Gamma^k_{ij} + \xi \Theta_{ij}{}^k + \mathcal{O}(\xi^2)$ with $\Theta_{ij}{}^k := B_i{}^k{}_{|j} + B_j{}^k{}_{|i} - B_{ij}{}^{|k}$ for the pure tangential components of Christoffel symbols to express second-order covariant derivatives like the Laplace operator Δ

in the thin film. Our analysis also indicates that the surface evolution equation can be derived directly without a detour of a global energy minimization problem. However, there is no general theory regarding sufficient prerequisites of this analysis, and we can not ensure, that, for example, every well-posed tensorial thin film problem results in a well-posed tensorial surface problem.

Even with the made approximations in the modelling approach, the numerical results provide new insights on the tight coupling of topology, geometry, and energetic minimal states as well as dynamics. In a next step, the derived coupling terms should be investigated systematically and the model should be validated versus experimental data. Various extensions of the proposed model, like coupling to hydrodynamics and/or activity open up a wide array of possible physical applications in material science or biophysics. For recent work on hydrodynamics on surfaces, we refer to [31,38–40]. Also investigations on energy minimization and dynamics on moving domains seem now feasible. However, to deal with these problems numerically requires a more detailed investigation of the regularity. In contrast to our assumption for the tensor fields to be sufficiently smooth, which was made for simplicity, tensorial Sobolev spaces should be investigated (e.g. [41]).

Data accessibility. This work does not have any experimental data.

Authors' contributions. I.N. conducted the thin film analysis. M.N. and S.P. implemented the model and performed finite-element simulations. M.N., S.P. and A.V. conceived and interpreted the numerical experiments. All authors contributed to a critical discussion of the derived model and numerical data and participated in writing the manuscript, which S.P. and A.V. finalized. H.L. and A.V. coordinated the project.

Competing interests. We have no competing interests.

Funding. H.L. and A.V. acknowledge the financial support from DFG through Lo481/20 and Vo899/19, respectively. We further acknowledge computing resources provided by JSC under grant HDR06 and ZIH/TU Dresden.

Appendix A

Lemma A.1. *For all surface q-Tensors $\boldsymbol{q} \in \mathcal{Q}(\mathcal{S})$ holds*

$$\int_{\mathcal{S}} \|\operatorname{div} \boldsymbol{q}\|^2 \, d\mathcal{S} = \int_{\mathcal{S}} \frac{1}{2}\|\nabla \boldsymbol{q}\|^2 + \mathcal{K}\operatorname{tr} \boldsymbol{q}^2 \, \mathrm{d}S \tag{A 1}$$

and

$$\int_{\mathcal{S}} \langle \nabla \boldsymbol{q}, (\nabla \boldsymbol{q})^{T_{(2\,3)}} \rangle \, d\mathcal{S} = \int_{\mathcal{S}} \frac{1}{2}\|\nabla \boldsymbol{q}\|^2 - \mathcal{K}\operatorname{tr} \boldsymbol{q}^2 \, \mathrm{d}S. \tag{A 2}$$

Proof. With the surface Levi–Civita tensor $\boldsymbol{E} \cong \mathrm{d}\mathcal{S}$ defined by

$$E_{ij} := \mathrm{d}\mathcal{S}(\partial_i \boldsymbol{x}, \partial_j \boldsymbol{x}) = \sqrt{\det \boldsymbol{g}}\,\varepsilon_{ij} \tag{A 3}$$

with Levi–Civita symbols ε_{ij}, we use the 2-tensor curl

$$[\operatorname{rot} \boldsymbol{q}]_i := [-\nabla \boldsymbol{q} : \boldsymbol{E}]_i = -E_{jk} q_i^{\ jk} \tag{A 4}$$

and observe

$$[-\boldsymbol{E} \cdot \operatorname{rot} \boldsymbol{q}]_i = E_{il}E_{jk}q^{lj|k} = (g_{ij}g_{lk} - g_{ik}g_{lj})q^{lj|k} = q^l{}_{i|l} - q^j{}_{j|i} = q_i{}^l{}_{|l} = [\operatorname{div} \boldsymbol{q}]_i. \tag{A 5}$$

Moreover, in this case, $-\boldsymbol{E}\cdot$ is isomorph to the Hodge-star operator $*$ on differential 1-forms and therefore it can be seen as a length preserving pointwise counterclock quarter turn, that is why $\|\operatorname{rot} \boldsymbol{q}\| = \| - \boldsymbol{E} \cdot \operatorname{rot} \boldsymbol{q}\| = \|\operatorname{div} \boldsymbol{q}\|$ holds for the norm. We remark that $\boldsymbol{E} \in \mathrm{T}^{(2)}\mathcal{S}$ is compatible with ∇ and hence, we calculate

$$\begin{aligned}\int_{\mathcal{S}} \|\operatorname{div} \boldsymbol{q}\|^2 \mathrm{d}\mathcal{S} &= \frac{1}{2}\int_{\mathcal{S}} \|\operatorname{div} \boldsymbol{q}\|^2 + \|\operatorname{rot} \boldsymbol{q}\|^2 \, \mathrm{d}\mathcal{S} = -\frac{1}{2}\int_{\mathcal{S}} (q_i^{\ k}{}_{|k|l} + E_{kj}E_{lm}q_i^{\ k|j|m})q^{il} \, \mathrm{d}\mathcal{S} \\ &= -\frac{1}{2}\int_{\mathcal{S}} (q_i^{\ k}{}_{|k|l} + q_{il}^{\ \ \ |j}{}_{|j} - q_i^{\ k}{}_{|l|k})q^{il} \, \mathrm{d}\mathcal{S}.\end{aligned} \tag{A 6}$$

The Riemannian curvature tensor has only one independent component on surfaces and is given by $\boldsymbol{R} = \mathcal{K}\boldsymbol{E} \otimes \boldsymbol{E} \in \mathrm{T}^{(4)}\mathcal{S}$. Hence, for changing the order of covariant derivatives, holds

$$q_i^{\ k}{}_{|k|l} - q_i^{\ k}{}_{|l|k} = R^j{}_{ikl} q_j^{\ k} - R^k{}_{jkl} q_i^{\ j} = \mathcal{K}((\delta^j{}_k g_{il} - \delta^j{}_l g_{ik}) q_j^{\ k} - (\delta^k{}_k g_{jl} - \delta^k{}_l g_{jk}) q_i^{\ j}) = -2\mathcal{K} q_{il}. \tag{A 7}$$

Finally, we get

$$\int_{\mathcal{S}} \|\mathrm{div}\boldsymbol{q}\|^2 \,\mathrm{d}\mathcal{S} = -\frac{1}{2}\int_{\mathcal{S}} (q_{il}{}^{|j}{}_{|j} - 2\mathcal{K} q_{il}) q^{il} \,\mathrm{d}\mathcal{S} = \int_{\mathcal{S}} \frac{1}{2}\|\nabla\boldsymbol{q}\|^2 + \mathcal{K}\mathrm{tr}\boldsymbol{q}^2 \,\mathrm{d}\mathcal{S} \tag{A 8}$$

and

$$\begin{aligned}\int_{\mathcal{S}} \langle \nabla\boldsymbol{q}, (\nabla\boldsymbol{q})^{T_{(23)}} \rangle \,\mathrm{d}\mathcal{S} &= -\int_{\mathcal{S}} q_i^{\ k}{}_{|l|k} q^{il} \,\mathrm{d}\mathcal{S} = -\int_{\mathcal{S}} (q_i^{\ k}{}_{|k|l} + 2\mathcal{K} q_{il}) q^{il} \,\mathrm{d}\mathcal{S} \\ &= \int_{\mathcal{S}} \|\mathrm{div}\boldsymbol{q}\|^2 - 2\mathcal{K}\mathrm{tr}\boldsymbol{q}^2 \,\mathrm{d}\mathcal{S} = \int_{\mathcal{S}} \frac{1}{2}\|\nabla\boldsymbol{q}\|^2 - \mathcal{K}\mathrm{tr}\boldsymbol{q}^2 \,\mathrm{d}\mathcal{S}.\end{aligned} \tag{A 9}$$

■

Lemma A.2. *For all 2-tensors $\boldsymbol{t} \in \mathrm{T}^{(2)}\mathcal{S}$ at surface $\mathcal{S}$ holds*

$$\boldsymbol{t}^2 = (\mathrm{tr}\,\boldsymbol{t})\boldsymbol{t} + \tfrac{1}{2}(\mathrm{tr}\,\boldsymbol{t}^2 - (\mathrm{tr}\,\boldsymbol{t})^2)\boldsymbol{g}. \tag{A 10}$$

Proof. With the surface Levi–Civita tensor $\boldsymbol{E}$ defined in (A 3), the quarter turn in the row and column space of a 2-tensor $\boldsymbol{t} \in \mathrm{T}^{(2)}\mathcal{S}$ is

$$[\boldsymbol{E}\boldsymbol{t}\boldsymbol{E}]_{ij} = E_{ik}E_{lj}t^{kl} = (g_{il}g_{kj} - g_{ij}g_{kl})t^{kl} = t_{ji} - t^k{}_k g_{ij} = [\boldsymbol{t}^T - (\mathrm{tr}\,\boldsymbol{t})\boldsymbol{g}]_{ij}. \tag{A 11}$$

Particularly, (A 11) is also valid for the square of $\boldsymbol{t}$, i.e.

$$\boldsymbol{E}\boldsymbol{t}^2\boldsymbol{E} = (\boldsymbol{t}^2)^{\mathrm{T}} - (\mathrm{tr}\,\boldsymbol{t}^2)\boldsymbol{g}. \tag{A 12}$$

On the other hand, with $\boldsymbol{E}\boldsymbol{E} = -\boldsymbol{g}$, (A 11) and $(\boldsymbol{t}^T)^2 = (\boldsymbol{t}^2)^{\mathrm{T}}$, we calculate

$$\begin{aligned}\boldsymbol{E}\boldsymbol{t}^2\boldsymbol{E} &= -(\boldsymbol{E}\boldsymbol{t}\boldsymbol{E})^2 = -(\boldsymbol{t}^T - (\mathrm{tr}\,\boldsymbol{t})\boldsymbol{g})^2 = -(\boldsymbol{t}^T)^2 + 2(\mathrm{tr}\,\boldsymbol{t})\boldsymbol{t}^T - (\mathrm{tr}\,\boldsymbol{t})^2\boldsymbol{g} \\ &= -(\boldsymbol{t}^2)^{\mathrm{T}} + 2(\mathrm{tr}\,\boldsymbol{t})\boldsymbol{E}\boldsymbol{t}\boldsymbol{E} + (\mathrm{tr}\,\boldsymbol{t})^2\boldsymbol{g}.\end{aligned} \tag{A 13}$$

Averaging identities (A 12) and (A 13) results in

$$\boldsymbol{E}\boldsymbol{t}^2\boldsymbol{E} = (\mathrm{tr}\,\boldsymbol{t})\boldsymbol{E}\boldsymbol{t}\boldsymbol{E} + \tfrac{1}{2}((\mathrm{tr}\,\boldsymbol{t})^2 - \mathrm{tr}\,\boldsymbol{t}^2)\boldsymbol{g}. \tag{A 14}$$

Finally, we obtain (A 10) by a quarter turn with $\boldsymbol{E}$ in the row and column space of (A 14). ■

Lemma A.3. *For all **full covariant** 2-tensors $\boldsymbol{t} \in \mathrm{T}^0_2\mathcal{S}$ on surface $\mathcal{S}$ holds*

$$(\mathrm{tr}\,\boldsymbol{t})^2 - \mathrm{tr}\,\boldsymbol{t}^2 = 2\frac{\det\,\boldsymbol{t}}{\det\,\boldsymbol{g}} = 2\det\,\boldsymbol{t}^\sharp, \tag{A 15}$$

where det *means the determinant of the matrix proxy.*

Proof. We can interpret $\boldsymbol{t}$ as its matrix proxy with components t_{ij} due to the stipulation of the height of the indices. Hence, the determinant can be calculated applying the Levi–Civita symbols $\varepsilon_{ij} \in \{-1, 0, 1\}$, i.e.

$$\det\,\boldsymbol{t} = \frac{1}{2}\sum_{i,j,k,l} \varepsilon_{ij}\varepsilon_{kl}t_{ik}t_{jl}. \tag{A 16}$$

With the Levi–Civita tensor defined in (A 3), we obtain the transformation property

$$E^{ij} = \frac{1}{\det\,\boldsymbol{g}}E_{ij} = \frac{1}{\sqrt{\det\,\boldsymbol{g}}}\varepsilon_{ij}. \tag{A 17}$$

Therefore, (A 16) results in

$$\det\,\boldsymbol{t} = \frac{\det\,\boldsymbol{g}}{2}E^{ij}E^{kl}t_{ik}t_{jl} = \frac{\det\,\boldsymbol{g}}{2}(g^{ik}g^{jl} - g^{il}g^{jk})t_{ik}t_{jl} = \frac{\det\,\boldsymbol{g}}{2}(t_i^{\ i}t_j^{\ j} - t_i^{\ j}t_j^{\ i}). \tag{A 18}$$

Additionally, we observe

$$\det \boldsymbol{t}^{\sharp} = \det(\boldsymbol{t} \cdot \boldsymbol{g}^{-1}) = \frac{\det \boldsymbol{t}}{\det \boldsymbol{g}}. \tag{A 19}$$

■

Corollary A.4. *For shape operator $\boldsymbol{B}$ and Q-tensor $\boldsymbol{q} \in \mathcal{Q}(\mathcal{S})$, the following identities are valid.*

$$\|\boldsymbol{B}\|^2 = \mathrm{tr}\boldsymbol{B}^2 = \mathcal{H}^2 - 2\mathcal{K}, \tag{A 20}$$

$$\boldsymbol{B}^2 = \mathcal{H}\boldsymbol{B} - \mathcal{K}\boldsymbol{g}, \tag{A 21}$$

$$\langle \boldsymbol{B}^2, \boldsymbol{q}\rangle = \mathcal{H}\langle \boldsymbol{B}, \boldsymbol{q}\rangle, \tag{A 22}$$

$$\boldsymbol{q}^2 = \tfrac{1}{2}(\mathrm{tr}\,\boldsymbol{q}^2)\boldsymbol{g}, \tag{A 23}$$

$$\|\boldsymbol{B}\boldsymbol{q}\|^2 = \tfrac{1}{2}(\mathrm{tr}\,\boldsymbol{q}^2)(\mathcal{H}^2 - 2\mathcal{K}) \tag{A 24}$$

and

$$\mathrm{tr}(\boldsymbol{B}\boldsymbol{q})^2 = \langle \boldsymbol{B}, \boldsymbol{q}\rangle^2 + \mathcal{K}\mathrm{tr}\,\boldsymbol{q}^2. \tag{A 25}$$

Proof. The proofs here are very straightforward with all the spadework above. (A 20) is a consequence of lemma A.3 for $\boldsymbol{B} \in \mathrm{T}^{(2)}\mathcal{S}$ and hence, we obtain also (A 21) with lemma A.2. As $\boldsymbol{q} \in \mathcal{Q}(\mathcal{S})$ is trace-free, we follow from (A 21) that $t\langle \boldsymbol{B}^2, \boldsymbol{q}\rangle = \mathcal{H}\langle \boldsymbol{B}, \boldsymbol{q}\rangle - 2\mathcal{K}\mathrm{tr}\,\boldsymbol{q}$ and therefore (A 22). Again, $\boldsymbol{q}$ is a Q-tensor and thus lemma A.2 results in (A 23). The shape operator $\boldsymbol{B}$ is self-adjoint, so with (A 23) we can calculate

$$\|\boldsymbol{B}\boldsymbol{q}\|^2 = \langle \boldsymbol{B}\boldsymbol{q}, \boldsymbol{B}\boldsymbol{q}\rangle = \langle \boldsymbol{B}^2, \boldsymbol{q}^2\rangle = \tfrac{1}{2}(\mathrm{tr}\,\boldsymbol{q}^2)\langle \boldsymbol{B}^2, \boldsymbol{g}\rangle = \tfrac{1}{2}(\mathrm{tr}\,\boldsymbol{q}^2)\mathrm{tr}\boldsymbol{B}^2 \tag{A 26}$$

and get (A 24) with (A 20). We note that $\langle \boldsymbol{B}, \boldsymbol{q}\rangle^2 = (\mathrm{tr}\boldsymbol{B}\boldsymbol{q})^2$. Therefore, lemma A.3 results in (A 25), because

$$(\mathrm{tr}(\boldsymbol{B}\boldsymbol{q}))^2 - \mathrm{tr}(\boldsymbol{B}\boldsymbol{q})^2 = 2\det(\boldsymbol{B}\boldsymbol{q})^{\sharp} = 2(\det \boldsymbol{B}^{\sharp})(\det \boldsymbol{q}^{\sharp}) = \mathcal{K}((\mathrm{tr}\,\boldsymbol{q})^2 - \mathrm{tr}\,\boldsymbol{q}^2) = -\mathcal{K}\mathrm{tr}\,\boldsymbol{q}^2. \tag{A 27}$$

■

Lemma A.5. *For the inverse thin film metric $\boldsymbol{G}^{-1}$ holds*

$$\left.\begin{aligned} G^{ij} &= \left(g^{ik} + \sum_{\mathfrak{l}=1}^{\infty} \xi^{\mathfrak{l}}[\boldsymbol{B}^{\mathfrak{l}}]^{ik}\right)\left(\delta^j_k + \sum_{\mathfrak{k}=1}^{\infty} \xi^{\mathfrak{k}}[\boldsymbol{B}^{\mathfrak{k}}]_k{}^j\right) \\ &= \left[\left(\boldsymbol{g} + \sum_{\mathfrak{k}=1}^{\infty} \xi^{\mathfrak{k}}\boldsymbol{B}^{\mathfrak{k}}\right)^2\right]^{ij}, \\ G^{\xi\xi} &= 1 \\ \text{and} \quad G^{i\xi} &= G^{\xi i} = 0. \end{aligned}\right\} \tag{A 28}$$

Proof. First, we define the pure tangential components of the thin film metric tensor as $\boldsymbol{G}_t := \{G_{ij}\}$. With $\boldsymbol{\delta} = \{\delta^i_j\}$ the Kronecker delta, we can write down in usual matrix notation

$$\boldsymbol{G} \cdot \boldsymbol{G}^{-1} = \begin{bmatrix} \boldsymbol{G}_t & O \\ O & 1 \end{bmatrix} \cdot \begin{bmatrix} \{G^{ij}\} & \{G^{i\xi}\} \\ \{G^{\xi i}\} & G^{\xi\xi} \end{bmatrix} = \begin{bmatrix} \boldsymbol{\delta} & O \\ O & 1 \end{bmatrix}. \tag{A 29}$$

Thus, we obtain

$$G^{\xi\xi} = 1, \tag{A 30}$$

$$G^{i\xi} = G^{\xi i} = 0 \tag{A 31}$$

and

$$\{G^{ij}\} = \boldsymbol{G}_t^{-1} = (\boldsymbol{g} - \xi\boldsymbol{B})^{-2} = (\boldsymbol{g} - \xi\boldsymbol{B})^{-1} \cdot (\boldsymbol{\delta} - \xi\boldsymbol{B}^{\sharp})^{-1}. \tag{A 32}$$

For h small enough, so that $\xi\|\boldsymbol{B}\| \leq h\|\boldsymbol{B}\| < 1$ and exponent with a dot indicate matrix (endomorphism) power, we can use the Neumann series

$$(\boldsymbol{\delta} - \xi \boldsymbol{B}^\sharp)^{-1} = \boldsymbol{\delta} + \sum_{\mathfrak{k}=1}^{\infty} \xi^{\mathfrak{k}} (\boldsymbol{B}^\sharp)^{\cdot \mathfrak{k}}, \tag{A 33}$$

and therefore the assertion, because with $\boldsymbol{B}^{\mathfrak{k}} = (\boldsymbol{B} \cdot \boldsymbol{g}^{-1})^{\cdot \mathfrak{k}} \cdot \boldsymbol{g}$ we get

$$(\boldsymbol{B}^\sharp)^{\cdot \mathfrak{k}} = (\boldsymbol{B} \cdot \boldsymbol{g}^{-1})^{\cdot \mathfrak{k}} = \boldsymbol{B}^{\mathfrak{k}} \cdot \boldsymbol{g}^{-1} = (\boldsymbol{B}^{\mathfrak{k}})^\sharp \tag{A 34}$$

and

$$(\boldsymbol{g} - \xi \boldsymbol{B})^{-1} = ((\boldsymbol{\delta} - \xi \boldsymbol{B}^\sharp) \cdot \boldsymbol{g})^{-1} = \boldsymbol{g}^{-1} \cdot (\boldsymbol{\delta} - \xi \boldsymbol{B}^\sharp)^{-1} \tag{A 35}$$

■

Lemma A.6. *For the determinant of the thin shell film tensor* det $\boldsymbol{G}$ *holds*

$$\det \boldsymbol{G} = (1 - \xi \mathcal{H} + \xi^2 \mathcal{K})^2 \det \boldsymbol{g}, \tag{A 36}$$

Proof. The mixed components are zero, so we get

$$\det \boldsymbol{G} = G_{\xi\xi} \det \boldsymbol{G}_t = \det \boldsymbol{G}_t. \tag{A 37}$$

Now, we define $\sqrt{\boldsymbol{G}_t^\sharp} := (\boldsymbol{g} - \xi \boldsymbol{B})^\sharp$ as a square root of $\boldsymbol{G}_t^\sharp$, because

$$\boldsymbol{G}_t^\sharp = ((\boldsymbol{g} - \xi \boldsymbol{B})^2)^\sharp = ((\boldsymbol{g} - \xi \boldsymbol{B})^\sharp (\boldsymbol{g} - \xi \boldsymbol{B}))^\sharp = (\boldsymbol{g} - \xi \boldsymbol{B})^\sharp (\boldsymbol{g} - \xi \boldsymbol{B})^\sharp = \left(\sqrt{\boldsymbol{G}_t^\sharp}\right)^2. \tag{A 38}$$

Hence, we can calculate

$$\det \boldsymbol{G} = \det \boldsymbol{G}_t = \det \boldsymbol{G}_t^\sharp \boldsymbol{g} = \det \boldsymbol{G}_t^\sharp \det \boldsymbol{g} = \det \sqrt{\boldsymbol{G}_t^\sharp}^2 \det \boldsymbol{g}. \tag{A 39}$$

For the determinant of $\sqrt{\boldsymbol{G}_t^\sharp}$, we regard that $\boldsymbol{g}^\sharp = \boldsymbol{\delta}$ is the Kronecker delta, so we obtain

$$\det \sqrt{\boldsymbol{G}_t^\sharp} = \det(\boldsymbol{g}^\sharp - \xi \boldsymbol{B}^\sharp) = (1 - \xi B_u{}^u)(1 - \xi B_v{}^v) - \xi^2 B_u{}^v B_v{}^u \tag{A 40}$$

$$= 1 - \xi(B_u{}^u + B_v{}^v) + \xi^2 (B_u{}^u B_v{}^v - B_u{}^v B_v{}^u) = 1 - \xi \operatorname{tr} \boldsymbol{B} + \xi^2 \det \boldsymbol{B}^\sharp \tag{A 41}$$

$$= 1 - \xi \mathcal{H} + \xi^2 \mathcal{K}. \tag{A 42}$$

■

Lemma A.7. *Let* $\boldsymbol{W}$ *be an arbitrary n-tensor in the thin film (with sufficient regularity), which vanish at the boundaries, i.e.* $\boldsymbol{W} \in \{\boldsymbol{\Psi} \in \mathrm{T}^{(n)}\mathcal{S}_h : \boldsymbol{\Psi} = 0 \text{ at } \partial\mathcal{S}_h\}$, *holds*

$$\boldsymbol{W}|_{\mathcal{S}} = \partial_\xi \boldsymbol{W}|_{\mathcal{S}} = \mathcal{O}(h^2). \tag{A 43}$$

Proof. We denote the boundary at $\xi = h/2$ by Υ^+ and Υ^- at $\xi = -h/2$, s.t. $\Upsilon^+ \cup \Upsilon^- = \partial\mathcal{S}_h$. Taylor expansions at the surface result in

$$0 = \boldsymbol{W}|_{\Upsilon^\pm} = \boldsymbol{W}|_{\mathcal{S}} \pm \frac{h}{2} \partial_\xi \boldsymbol{W}|_{\mathcal{S}} + \frac{h^2}{8} \partial_\xi^2 \boldsymbol{W}|_{\mathcal{S}} + \mathcal{O}(h^3). \tag{A 44}$$

And we yield

$$0 = \boldsymbol{W}|_{\Upsilon^+} + \boldsymbol{W}|_{\Upsilon^-} = 2\boldsymbol{W}|_{\mathcal{S}} + \mathcal{O}(h^2) \tag{A 45}$$

and

$$0 = \boldsymbol{W}|_{\Upsilon^+} - \boldsymbol{W}|_{\Upsilon^-} = h \partial_\xi \boldsymbol{W}|_{\mathcal{S}} + \mathcal{O}(h^3). \tag{A 46}$$

■

References

1. Jenekhe SA, Chen XL. 1998 Self-assembled aggregates of rod-coil block copolymers and their solubilization and encapsulation of fullerenes. *Science* **279**, 1903–1907. (doi:10.1126/science.279.5358.1903)
2. Zerrouki D, Rotenberg B, Abramson S, Baudry J, Goubault C, Leal-Calderon F, Pine DJ, Bibette J. 2006 Preparation of doublet triangular, and tetrahedral colloidal clusters by controlled emulsification. *Langmuir* **22**, 57–62. (doi:10.1021/la051765t)
3. Keber FC, Loiseau E, Sanchez T, DeCamp SJ, Giomi L, Bowick MJ, Marchetti MC, Dogic Z, Bausch AR. 2014 Topology and dynamics of active nematic vesicles. *Science* **345**, 1135–1139. (doi:10.1126/science.1254784)
4. Dzubiella J, Schmidt M, Löwen H. 2000 Topological defects in nematic droplets of hard spherocylinders. *Phys. Rev. E* **62**, 5081–5091. (doi:10.1103/PhysRevE.62.5081)
5. Bates MA, Skacej G, Zannoni C. 2010 Defects and ordering in nematic coatings on uniaxial and biaxial colloids. *Soft Matter* **6**, 655–663. (doi:10.1039/B917180K)
6. Shin H, Bowick MJ, Xing X. 2008 Topological defects in spherical nematics. *Phys. Rev. Lett.* **101**, 037802. (doi:10.1103/PhysRevLett.101.037802)
7. Lopez-Leon T, Koning V, Devaiah KBS, Vitelli V, Fernandez-Nieves A. 2011 Frustrated nematic order in spherical geometries. *Nat. Phys.* **7**, 391–394. (doi:10.1038/nphys1920)
8. Lopez-Leon T, Fernandez-Nieves A, Nobili M, Blanc C. 2011 Nematic-smectic transition in spherical shells. *Phys. Rev. Lett.* **106**, 247802. (doi:10.1103/PhysRevLett.106.247802)
9. Dhakal S, Solis FJ, Olvera De La Cruz M. 2012 Nematic liquid crystals on spherical surfaces: control of defect configurations by temperature, density, and rod shape. *Phys. Rev. E* **86**, 011709. (doi:10.1103/PhysRevE.86.011709)
10. Koning V, Lopez-Leon T, Fernandez-Nieves A, Vitelli V. 2013 Bivalent defect configurations in inhomogeneous nematic shells. *Soft Matter* **9**, 4993–5003. (doi:10.1039/C3SM27671F)
11. Prinsen P, vanderSchoot P. 2003 Shape and director-field transformation of tactoids. *Phys. Rev. E* **68**, 021701. (doi:10.1103/PhysRevE.68.021701)
12. Selinger RLB, Konya A, Travesset A, Selinger JV. 2011 Monte Carlo studies of the XY model on two-dimensional curved surfaces. *J. Phys. Chem. B* **115**, 13 989–13 993. (doi:10.1021/jp205128g)
13. Nguyen TS, Geng J, Selinger RLB, Selinger JV. 2013 Nematic order on a deformable vesicle: theory and simulation. *Soft Matter* **9**, 8314–8326. (doi:10.1039/C3SM50489A)
14. Martinez A, Ravnik M, Lucero B, Visvanathan R, Zumer S, Smalyukh II. 2014 Mutually tangled colloidal knots and induced defect loops in nematic fields. *Nat. Mater.* **13**, 258–263. (doi:10.1038/nmat3840)
15. Segatti A, Snarski M, Veneroni M. 2014 Equilibrium configurations of nematic liquid crystals on a torus. *Phys. Rev. E* **90**, 012501. (doi:10.1103/PhysRevE.90.012501)
16. Alaimo F, Köhler C, Voigt A. 2017 Curvature controlled defect dynamics in topological active nematics. *Sci. Rep.* **7**, 5211. (doi:10.1038/s41598-017-05612-6)
17. Virga. EG. 1994 *Variational theories for liquid crystals*. London, UK: Chapman & Hall.
18. Stewart IW. 2004 *The static and dynamic continuum theory of liquid crystals: a mathematical introduction*. Boca Raton, FL: CRC Press.
19. Ball JM. 2017 Mathematics and liquid crystals. *Mol. Cryst. Liquid. Cryst.* **647**, 210–252. (doi:10.1080/15421406.2017.1289425)
20. Kralj S, Rosso R, Virga EG. 2011 Curvature control of valence on nematic shells. *Soft Matter* **7**, 670–683. (doi:10.1039/C0SM00378F)
21. Napoli G, Vergori L. 2012 Surface free energies for nematic shells. *Phys. Rev. E* **85**, 061701. (doi:10.1103/PhysRevE.85.061701)
22. Golovaty D, Montero JA, Sternberg P. 2017 Dimension reduction for the Landau–de Gennes model on curved nematic thin films. *J. Nonlinear Sci.* **27**, 1905–1932. (doi:10.1007/s00332-017-9390-5)
23. Canevari G, Segatti A. 2016 Defects in nematic shells: a Γ-convergence discrete-to-continuum approach. (http://arxiv.org/abs/1612.07720)
24. Mottram NJ, Newton CJP. 2014 Introduction to Q-tensor theory. (http://arxiv.org/abs/1409.3542)
25. Schiele K, Trimper S. 1983 On the elastic constants of a nematic liquid crystal. *Phys. Status Solidi B* **118**, 267–274. (doi:10.1002/pssb.2221180132)
26. Berreman DW, Meiboom S. 1984 Tensor representation of (o)seen-(f)rank strain energy in uniaxial cholesterics. *Phys. Rev. A* **30**, 1955–1959. (doi:10.1103/PhysRevA.30.1955)

27. Lubensky TC. 1970 Molecular description of nematic liquid crystals. *Phys. Rev. A* **2**, 2497–2514. (doi:10.1103/PhysRevA.2.2497)
28. Longa L, Monselesan D, Trebin H-R. 1987 An extension of the Landau-Ginzburg-de Gennes theory for liquid crystals. *Liq. Cryst.* **2**, 769–796. (doi:10.1080/02678298708086335)
29. Ball JM, Majumdar A. 2010 Nematic liquid crystals: from Maier-Saupe to a continuum theory. *Mol. Cryst. Liquid Cryst.* **525**, 1–11. (doi:10.1080/15421401003795555)
30. Nestler M, Nitschke I, Praetorius S, Voigt A. 2017 Orientational order on surfaces—the coupling of topology, geometry, and dynamics. *J. Nonlinear Sci.* **28**, 147–191. (doi:10.1007/s00332-017-9405-2)
31. Reuther S, Voigt A. 2018 Solving the incompressible surface Navier-Stokes equation by surface finite elements. *Phys. Fluids* **30**, 012107. (doi:10.1063/1.5005142)
32. Dziuk G, Elliott CM. 2013 Finite element methods for surface PDEs. *Acta Numer.* **22**, 289–396. (doi:10.1017/S0962492913000056)
33. Vey S, Voigt A. 2007 AMDiS: adaptive multidimensional simulations. *Comput. Vis. Sci.* **10**, 57–67. (doi:10.1007/s00791-006-0048-3)
34. Witkowski T, Ling S, Praetorius S, Voigt A. 2015 Software concepts and numerical algorithms for a scalable adaptive parallel finite element method. *Adv. Comput. Math.* **41**, 1145–1177. (doi:10.1007/s10444-015-9405-4)
35. Lubensky TC, Prost J. 1992 Orientational order and vesicle shape. *J. Phys. II* **2**, 371–382. (doi:10.1051/jp2:1992133)
36. Nelson DR. 2002 Towards a tetravalent chemistry of colloids. *Nano Lett.* **2**, 1125–1129. (doi:10.1021/nl0202096)
37. Iyer G, Xu X, Zarnescu AD. 2015 Dynamic cubic instability in a 2D Q-tensor model for liquid crystals. *Math. Mod. Methods Appl. Sci.* **25**, 1477–1517. (doi:10.1142/S0218202515500396)
38. Nitschke I, Voigt A, Wensch J. 2012 A finite element approach to incompressible two-phase flow on manifolds. *J. Fluid Mech.* **708**, 418–438. (doi:10.1017/jfm.2012.317)
39. Reuther S, Voigt A. 2015 The interplay of curvature and vortices in flow on curved surfaces. *Multiscale Model. Sim.* **13**, 632–643. (doi:10.1137/140971798)
40. Nitschke I, Reuther S, Voigt A. 2017 Discrete exterior calculus (DEC) for the surface Navier-Stokes equation. In *Transport processes at fluidic interfaces* (eds D Bothe, A Reusken), pp. 177–197. Berlin, Germany: Springer.
41. Segatti A, Snarski M, Veneroni M. 2016 Analysis of a variational model for nematic shells. *Math. Mod. Methods. Appl. Sci.* **26**, 1865–1918. (doi:10.1142/S0218202516500470)